3．HIVの感染事例

日本でHIVは，①(特に男性)同性愛者に多く感染・発症し，②適切な薬物療法等を実施しないと，最終的にAIDSを発症し致死的となる，③非加熱の血液製剤を介して約4割の血友病患者が感染し薬害AIDS訴訟に発展した，などと言ったことから非常に注目を浴びた。そのため未知のウイルスであったにもかかわらず，感染事例報告から対策までの期間が相対的に短かった。HIV感染事例は，未知の感染性因子が新興感染症として血液を介して感染したという事例であり，血液や血液製剤の安全性確保が重要な課題であることを広く社会に知らしめる結果をもたらした。

4．HCVの感染事例

1964年，米国のライシャワー駐日大使(当時)が暴漢に襲われ，輸血を伴う緊急手術を受けるという事件が発生した。この輸血用血液が有償血液(いわゆる売血)であり，HCVに汚染されていたため，ライシャワー氏は肝炎を発症し最終的には肝細胞癌を発症し亡くなった。この事件を機に1962年から始まっていた「黄色い血追放キャンペーン」が大きな反響を呼び，売血制度の撤廃と国内献血制度の確立に至っている。前述のように，輸血後肝炎の第一のターゲットはHBVだったが，このHCV対策をもって，実質上輸血後肝炎の発症は収束に向かったと言える。

一方，肝炎ウイルスによる感染事例はいくつかの血漿分画製剤によっても起きた。**表1**に主なHCV感染事例と感染防止対策を示す。

表1　HCVによる感染事例と感染防止対策

西暦	出来事
1964	㈱日本ブラッドバンクの「フィブリノーゲン」製造承認
1965	弛緩出血ショック止血措置輸血措置懈怠による事件 DICの妊婦にフィブリノゲンを投与せず死亡
1974	「C型肝炎」の存在が提唱される
1975	弛緩出血ショック止血措置輸血措置懈怠による事件， 担当医師が敗訴となる
1977	米国FDA，フィブリノゲン製剤の承認取り消し
	青森で非加熱フィブリノゲン製剤による肝炎集団感染発生
1987	加熱フィブリノゲン製剤を製造承認
	非加熱フィブリノゲン製剤の適応を先天性疾患に限定
1988	米カイロン社，HCVのウイルス遺伝子クローニングに一部成功
1989	HCV抗体検査法(第一世代)導入
1992	HCV抗体検査法(第二世代)導入
1994	静注用グロブリン製剤「ガンマーガード」によるHCV感染と自主回収

(1)非加熱のフィブリノゲンの事例

1965年，DIC*4を合併した妊婦が弛緩出血ショックを発症した。この際，担当医師は適切に輸血せず患者を死亡させたとして訴訟に発展した。10年後，この担当医師は輸血措置懈怠として敗訴したため，これ以降，日本では出血のリスクがある妊婦に対して，輸血よりも止血効率の高い静注用フィブリノゲン製剤の投与が標準化した。しかし，この静注用フィブリノゲン製剤は，当時ウイルスを不活化するための加熱処理が行われていなかった。1977年，FDAは非加熱フィブリノゲン製剤による感染リスクを認識し承認を取り消したが，わが国では1987年，青森で肝炎集団感染が起きるまで具体的な施策はなかった。この間，非加熱フィブリノゲン製剤を投与された妊婦は肝炎ウイルスに感染した可能性が高く，いわゆる薬害肝炎訴訟，肝炎対策基本法の成立に至っている。

*4播種性血管内凝固症候群(disseminated intravascular coagulation syndrome)。全身の血管内に広範かつ持続性の微小血栓が多発する疾患。進行すると微小循環障害によって臓器障害を来すとともに，血小板や凝固因子が消費され，血栓症であるにもかかわらず出血症状が出現する。この場合，凝固因子補充のため輸血や静注用フィブリノゲン製剤が使用される。

(2)静注用免疫グロブリン製剤の事例

C型肝炎ウイルスが発見され，肝炎発症が終息しつつあった1994年，静注用の免疫グロブリン製剤で200例規模のHCV感染事例が発生した。1989年以降，製剤の原料血漿はすべてHCVに汚染されていないか酵素免疫測定法(EIA：enzyme immunoassay)で測定し，陰性を確認して使われていたが，非構造領域のNS4領域の一部(C100-3)を抗原とする抗体測定系(第一世代)を経て，C100-3抗原，コア抗原，NS3領域の抗原を組み合わせて検出感度を上げた第二世代抗体測定系を導入したその年の1994年に，結果として感染事故が発生したという。この一見矛盾する事例は，第一世代では検査をすり抜けて原料血漿に残存していた抗HCV抗体が混入していたウイルスを中和していたが，第二世代では抗HCV抗体を含む原料血漿がほぼ完全に取り除かれた結果，混入していたウイルスが中和されず，以降の精製工程へ進んだことが原因と考えられている。さらにこの製剤の製造プロセスには，このウイルスを十分に除去，不活化できる工程が含まれなかったことも重大な原因と考えられている。事故発生直後，メーカーはこの製剤を自主回収，承

認を取り下げ，ウイルス不活化工程を導入した安全な製剤に切り替えた。

5．HPV-B19の感染事例

HPV-B19は，伝染性紅斑の原因ウイルスとして知られる。このウイルスは上述３ウイルス（HBV，HIVおよびHCV）とは異なり致死的ではなく，実際日本人の過半数が感染既往を示す抗体陽性である。しかし，妊婦に感染した場合，胎児水腫や死産のリスクがあることから，原料血漿のスクリーニング対象となっている。さらにスクリーニングの基準も他の３ウイルスとは異なる。すなわち，他の３ウイルスは検出できないことを前提としたスクリーニングであるのに対し，HPV-B19では，原料となるプール血漿で10^4IU/mLを超えなければ製造に用いることができるとFDAは勧告している。この10^4IU/mLの設定値については，以下のウイルス学的調査に基づいた背景がある。すなわち，1990年代後半に製造された血漿分画製剤，S/D処理血漿の多くはHPV-B19に汚染されており，実際に感染事例が報告されている。これら感染を引き起こした製剤中のウイルス量を調査することから，感染した製剤中のウイルス濃度下限が判明している。これを根拠として，原料血漿中のウイルス濃度を逆算し，FDAはこの勧告を発出した。本邦でも基本的にFDAガイドラインに準拠している。もちろん，各血漿分画製剤の製造プロセスには不活化，除去工程が含まれ，製品は最終的にNATで陰性であることを確認して出荷されている。

HPV-B19のように，安全対策上の感染リスクが定量的に明らかである場合は，スクリーニングの時点で必ずしもすべて排除する必要はないと考えられている。なお，HPV-B19に汚染された血漿をすべて排除できないもう１つの理由は，前述のように国民の多くが感染既往で，比較的高頻度にB19-DNAが検出されるためであり，NATのような検出感度の高い検出システムですべての血漿を排除すると原料血漿が不足し，製剤を供給できなくなるためである。

6．感染事例から学んだこと

４つのウイルスの感染事例を通して学んだことは下記である。

①ウイルスの感染事例・対策の経緯は，製剤による感染事例報告，ウイルスの発見，ウイルス汚染対策（スクリーニングの導入）であり，感染被害拡大を抑制するためには感染情報から対策までの期間を短縮することが重要である。

②ウイルス汚染対策のしくみ，技術が向上し，想定されるウイルスに対してその安全性が向上した。具体的にはウイルススクリーニング，ウイルスクリアランス，ウイルスモニタリングである。

感染情報から対策までの期間を短縮することは重要だが限界がある。そのため，汚染対策の仕組み，技術が重要である。ウイルススクリーニングは，ドナーである供血者の問診，血液検査，ウイルス抗原検査，ウイルス抗体検査，NAT，および６カ月間の貯留保管を組み合わせることで行われている。ウイルスクリアランスは，主に２つのアプローチで製造工程に取り入れられている。１つはウイルスを不活化する工程，もう１つはウイルスを除去する工程で，異なる２つ以上の工程で，遡及調査に伴い，陽性となった血漿の原料への混入が判明した場合，製造工程において当該ウイルスのウイルスクリアランス値が９ログ以上であれば当該製剤を回収する必要はないとされている。ウイルスモニタリングでは，感染症定期報告，副作用・感染症報告，遡及調査がある。特に感染症定期報告制度は，薬事法第68条，および血液法*5で規定される制度で，「製剤の原料もしくは材料による感染症に関する最新の論文その他により得られた知見に基づき当該生物由来製品を評価しその成果を厚生労働大臣に定期的に報告」する制度である。血液製剤の場合は，薬事・食品衛生審議会に報告，審議される。すなわち，感染症の発生頻度や傾向などを把握するため，原料であるヒトに発生した感染症はもちろん，動物由来材料が使われる場合を考慮し，関連する動物に発生した感染症に

1. 原料血液のウイルススクリーニング
   - 問診，血液検査（ALT（GPT），AST（GOT）等），ウイルス抗原検査（HBs抗原，B19抗原），ウイルス抗体検査（HBs抗体，HBc抗体等），核酸増幅検査（HIV，HBV，HCV，HAV，HPV-B19），貯留保管（6カ月）
2. ウイルスクリアランス工程
   - ウイルス不活化工程
     - 加熱処理工程
       - 液状加熱処理，乾燥加熱処理，HTST*等
     - 有機溶媒／界面活性剤処理（S/D処理）
   - ウイルス除去工程
     - 沈殿分画法
     - ウイルス除去膜
3. ウイルス情報の監視活動（モニタリング）
   - 感染症定期報告，遡及調査，副作用・感染症報告

* HTST：High temperature short time method sterilization（高温短時間殺菌法）

図7　ウイルス対策の3本柱

ついても最新の知見を常に把握し，感染症のリスクを多角的に評価・検討，これらの情報が集積されている（図7）。

*5安全な血液製剤の安定供給の確保等に関する法律

まとめ

以上述べたような分科会の検討を通じて，①過去のウイルス感染事例とその汚染対策技術の進歩により安全性が向上している，②ウイルスの発生情報を監視する制度が整備され常時モニターされている，という現状を確認した。今後もウイルス汚染リスクを考慮し，継続して危険性に注意を払っていく必要がある。ICH Q9ガイドラインでは，品質リスクマネジメントとしてマネジメントプロセスを提示している。ガイドラインの典型的なマネジメントプロセスを示した図を基本に，リスクをウイルスリスクと変換して作図した（図8）。本稿で述べたように，これまで血液製剤，血漿分画製剤では不幸にも重大な感染事故が発生したが，国と血液事業者が協力してさまざまな対策が講じられた結果，ことウイルスリスクマネジメントのプロセスとしては，事象レビューまで含めて，一定のレベルまで達成できていると評価できよう。一方，スクリーニング，クリアランス，モニタリングといったマネジメントプロセスの各パーツはあったとしても，十分機能しているか，あるいはそれらが国と各血液事業者，あるいは事業者間の組織体の中で有機的に連携しているか（コミュニケーション）という点ではまだ課題が残るとの意見もあった。今後分科会としてマネジメントプロセスの観点で，製剤のさらなる安全性向上のために検討を継続したい。

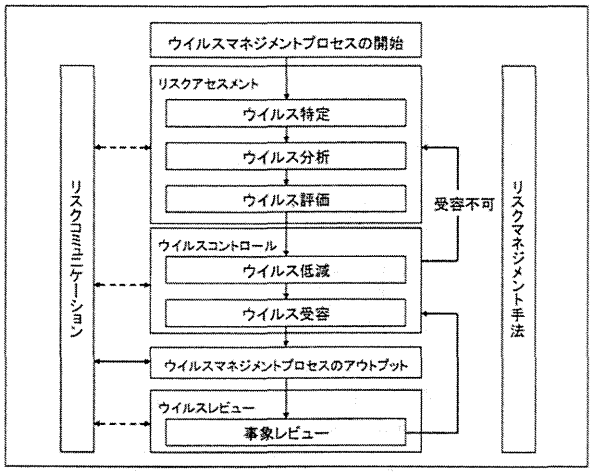

図8 ウイルスリスクマネジメントの概念図

■参考文献

1) Tabor E.：“The epidemiology of virus transmission by plasma derivatives：clinical studies verifying the lack of transmission of hepatitis B and C viruses and HIV type 1.” *TRANSFUSION*, **39**, 1160-1168(1999)
2) Yu, M.Y., Bartosch, B., Zhang, P., Guo, Z.P., Renzi, P.M., Shen, L.M., Granier, C., Feinstone, S.M., Cosset, F.L., Purcell, R.H.：Neutralizing antibodies to hepatitis C virus (HCV) in immune globulins derived from anti-HCV-positive plasma. Proc. *Natl. Acad. Sci. USA.*, **101**, 7705-7710(2004)
3) 厚生労働省ホームページ（平成22年度第1回薬事・食品衛生審議会血液事業部会安全技術調査会および平成22年度第3回薬事・食品衛生審議会医薬品等安全対策部会安全対策調査会（合同開催）），http://www.mhlw.go.jp/shingi/2010/06/dl/s0623-20m.pdf,（accessed 2013-3-3）
4) Guidance for Industry：Nucleic Acid Testing (NAT) to Reduce the Possible Risk of Parvovirus B19 Transmission by Plasma-Derived Products, U.S. Department of Health and Human Services Food and Drug Administration, Center for Biologics Evaluation and Research July 2009
5) Brown KE, Young NS, Alving BM, Barbosa LH.：Parvovirus B19：implications for transfusion medicine. Summary of a workshop, *TRASFUSION*, **41**, 130-135(2001)
6) 日本赤十字社ホームページ医薬品情報：血液製剤の安全性の向上についてhttp://www.jrc.or.jp/vcms_lf/iyakuhin_yuketu081125.pdf,（accessed 2013-3-2）
7) バイオ医薬品ハンドブック～Biologicsの製造から品質管理まで～，日本PDA製薬学会 バイオウイルス委員会編，2012年，じほう

日本PDA製薬学会 バイオウイルス委員会 SALLY分科会メンバー

亀井慎太郎[1]，井上雅晴[2]，大和田尚[3]，岡野 清[4]，小田昌宏[5]，川俣 治[6]，北野 誠[7]，洪 苑起[8]，小杉公彦[9]，塩見哲次[10]，末永正人[11]，菅谷真二[12]，菅原敬信[1]，龍田祐治[13]，築山美奈[14]，松野哲巌[15]，丸山裕一[16]，村井活史[17]，新見伸吾[18]

一般財団法人化学及血清療法研究所[1]，旭化成メディカル株式会社[2]，日本赤十字社中央血液研究所[3]，株式会社東レリサーチセンター[4]，日本ポール株式会社[5]，株式会社エスアールエル[6]，ディー・エス・エムジャパン株式会社[7]，日本製薬株式会社[8]，日本ミリポア株式会社[9]，和光純薬工業株式会社[10]，武田薬品工業株式会社[11]，東和薬品株式会社[12]，東洋紡バイオロジックス株式会社[13]，日本チャールス・リバー株式会社[14]，旭化成ファーマ株式会社[15]，デンカ生研株式会社[16]，一般社団法人日本血液製剤機構[17]，国立医薬品食品衛生研究所[18]

PLOS ONE

Structure and Dynamics of the gp120 V3 Loop That Confers Noncompetitive Resistance in R5 HIV-1_{JR-FL} to Maraviroc

Yuzhe Yuan[1], Masaru Yokoyama[2], Yosuke Maeda[3], Hiromi Terasawa[3], Shinji Harada[3], Hironori Sato[2], Keisuke Yusa[4]*

1 Transfusion Transmitted Diseases Center, Institute of Blood Transfusion, Chinese Academy of Medical Science, Chenghua District, Chengdu, Sichuan Province, P. R. China, **2** Pathogen Genomics Center, National Institute of Infectious Diseases, Musashi Murayama, Tokyo, Japan, **3** Department of Medical Virology, Graduate School of Medical Sciences, Kumamoto University, Kumamoto, Japan, **4** Division of Biological Chemistry and Biologicals, National Institute of Health Sciences, Setagaya, Tokyo, Japan

Abstract

Maraviroc, an (HIV-1) entry inhibitor, binds to CCR5 and efficiently prevents R5 human immunodeficiency virus type 1 (HIV-1) from using CCR5 as a coreceptor for entry into $CD4^+$ cells. However, HIV-1 can elude maraviroc by using the drug-bound form of CCR5 as a coreceptor. This property is known as noncompetitive resistance. HIV-$1_{V3\text{-}M5}$ derived from HIV-$1_{JR\text{-}FLan}$ is a noncompetitive-resistant virus that contains five mutations (I304V/F312W/T314A/E317D/I318V) in the gp120 V3 loop alone. To obtain genetic and structural insights into maraviroc resistance in HIV-1, we performed here mutagenesis and computer-assisted structural study. A series of site-directed mutagenesis experiments demonstrated that combinations of V3 mutations are required for HIV-$1_{JR\text{-}FLan}$ to replicate in the presence of 1 μM maraviroc, and that a T199K mutation in the C2 region increases viral fitness in combination with V3 mutations. Molecular dynamic (MD) simulations of the gp120 outer domain V3 loop with or without the five mutations showed that the V3 mutations induced (i) changes in V3 configuration on the gp120 outer domain, (ii) reduction of an anti-parallel β-sheet in the V3 stem region, (iii) reduction in fluctuations of the V3 tip and stem regions, and (iv) a shift of the fluctuation site at the V3 base region. These results suggest that the HIV-1 gp120 V3 mutations that confer maraviroc resistance alter structure and dynamics of the V3 loop on the gp120 outer domain, and enable interactions between gp120 and the drug-bound form of CCR5.

Citation: Yuan Y, Yokoyama M, Maeda Y, Terasawa H, Harada S, et al. (2013) Structure and Dynamics of the gp120 V3 Loop That Confers Noncompetitive Resistance in R5 HIV-$1_{JR\text{-}FL}$ to Maraviroc. PLoS ONE 8(6): e65115. doi:10.1371/journal.pone.0065115

Editor: Jean-Pierre Vartanian, Institut Pasteur, France

Received February 14, 2013; **Accepted** April 21, 2013; **Published** June 28, 2013

Funding: This work was supported by grants from the Ministry of Health, Labour and Welfare and by the Global COE program Education and Research Center Aiming at the Control of AIDS from the Ministry of Education, Science, Sports and Culture, Japan. Y.Y. was supported by National Natural Science Foundation of China (81201329), scholarship for youth from Chinese Academy of Medical Sciences and Peking Union Medical College. The funders had no role in study design, data collection and analysis, decision to publish, or preparation of the manuscript.

Competing Interests: The authors have declared that no competing interests exist.

* E-mail: yusak@nihs.go.jp

Introduction

Inhibiting the entry of R5 human immunodeficiency virus type 1 (HIV-1) into $CCR5^+/CD4^+$ cells is an effective step in blocking viral replication. An entry inhibitor can bind to CCR5 and prevent R5 HIV-1 from using CCR5 as a coreceptor for entry [1]. Maraviroc, a CCR5 antagonist, has potent *in vitro* and *in vivo* antiviral activity against laboratory strains and clinical isolates [2–4]. Maraviroc, approved in 2007, was the first CCR5 antagonist approved by the US Food and Drug Administration and is currently used to treat patients with R5-tropic HIV-1 infections.

Treatment failures can occur because of an increasing number of pre-existing CXCR4-using viruses [5,6]. Alternatively, escape mutants can evade a CCR5 inhibitor by accumulating multiple mutations in gp120 and/or gp41 without switching their coreceptor usage [7–14]. Escape mutants can use the drug-bound form of CCR5 as a coreceptor, a property known as noncompetitive resistance [8,9,11]. In noncompetitive-resistant viruses, drug-free CCR5 usage is compatible with the additional ability of drug-bound CCR5 usage. We previously reported that a combination of polymorphic mutations in the gp120 V3 loop can confer noncompetitive resistance in HIV-$1_{JR\text{-}FL}$ [15]. One of these viruses, designated HIV-$1_{V3\text{-}M5}$, contains a set of five mutations I304V/F312W/T314A/E317D/I318V in the V3 loop (from Cys^{293} to Cys^{327}). Most other noncompetitive-resistant viruses contain multiple mutations in the V3 loop [8,9,11], although mutations reported till date in the V3 loop are not always common and resistance-associated mutations in the V3 loop were considered to be background dependent. Two elements are involved in gp120 coreceptor binding: (i) the V3 tip for the CCR5 extracellular loop 2 (ECL2) and (ii) the V3 base and stem residues and the V3 base of the gp120 core for the CCR5 N terminus [16–19]. Thus, the V3 loop of HIV-1 plays a pivotal role in its interaction with CCR5. However, how the V3 mutations induce maraviroc-resistance without changing coreceptor tropism remains unknown.

Increasing evidence indicates that the protein surface fluctuates in solution, and that such fluctuations play key roles in interactions with other molecules [20][20,23]. We previously suggested that the structural dynamics of the HIV-1 gp120 V3 loop play key roles

in modulating viral interactions with various molecules, including HIV-1 coreceptors and anti-V3 antibodies [21,22]. Therefore, it is conceivable that the V3 mutations that cause changes in the structural dynamics of the V3 loop may also be important for viral interactions with the maraviroc and CCR5 complex.

In this study, we examined how the V3 mutations, which conferred maraviroc resistance in HIV-1_{JR-FL}, affect the structural dynamics of the V3 loop on the gp120 outer domain. We initially performed extensive mutagenesis on the V3 loop to clarify a genetic basis for maraviroc-resistance of the HIV-1_{JR-FL} strain. These studies demonstrated that combinations of V3 mutations are required to render maraviroc resistance to HIV-1_{JR-FL}. Subsequently, we performed MD simulations [23–25] of HIV-1_{JR-FL} gp120 outer domains carrying V3 loops with and without the five maraviroc resistance mutations. The results illustrate that at the atomic-level maraviroc resistance mutations affect intrinsic structural properties and motion of the V3 loop on the HIV-1 gp120 outer domain.

Materials and Methods

Cells and Viruses

PM1/CCR5 cells were generated from the human $CD4^+$ T-cell line PM1 [26] by standard retrovirus-mediated transduction with pG1TKneo-CCR5 [27]. The cells were maintained in RPMI 1640 (Invitrogen) supplemented with 10% heat-inactivated fetal calf serum (FCS; Vitromex). MAGIC-5 cells (HeLa-$CD4^+$-$CCR5^+$-LTR-b-galactosidase) [28], used as reporter cells for HIV-1 infection, and 293T cells were maintained in Dulbecco's modified Eagle's medium (ICN Biomedicals) supplemented with 10% heat-inactivated FCS. pJR-FL was kindly provided by Prof. Koyanagi (Kyoto University).

MD simulation

HIV-1 gp120 outer domain structures with various V3 regions were constructed by the homology modeling method, using Molecular Operating Environment (MOE) software v. 2010.10 (Chemical Computing Group Inc., Montreal, Quebec, Canada) [22]. For the modeling template, we used the crystal structure of HIV-1 gp120 containing an entire V3 region at a resolution of 3.30 Å (PDB code: 2QAD) [29]. The 186 amino-terminal and 27 carboxyl-terminal residues were deleted to construct the gp120 outer domain structure. MD simulations were performed using the SANDER module of the AMBER 9 program package [30], the AMBER99SB force field [31], and the TIP3P water model [32]. Bond lengths involving hydrogen were constrained using SHAKE algorithm [32] and the time for all MD simulations was set to 2 fs. A nonbonded cutoff of 12 Å was used. After heating calculations for 20 ps until 310 K using the NVT ensemble, simulations were conducted with the NPT ensemble at 1 atm and 310 K for 20 ns. Superimposition of structures was performed by coordinating the atoms of the amino acids along the β-sheet at the gp120 core. We calculated the root mean square fluctuation (RMSF) to determine the atomic fluctuations along the trajectory broken down by residues during MD simulations. Average structures during the final 10 ns of MD simulations were used as reference structures. RMSFs were calculated using the ptraj module of AMBER 9 [22].

V3 mutant viruses

V3 mutant proviruses were constructed from pJR-FL_{an}. The 176-bp DNA fragments containing single mutations (I304V, F312W, T314A, E317D, or I318V) were subcloned into a cloning vector by overlapping PCR using primers tagged with a mutated tail. The mutation-containing DNA fragments encoding the V3 loop were repeatedly amplified from the cloning vectors using the primers VV-Af (5′-ACAGCTTAAGGAATC TGTAGAAAT-TAATTG-3′) and VV-Nh (5′-ATTTGCTAGCTATC TGTTTTAAAGTGTCAT-3′). Products were digested with AflII and NheI, subcloned into pCR-SXΔAN, and designated as pCR-SX_1, pCR-SX_2, pCR-SX_3, pCR-SX_4, and pCR-SX_5. The *Stu* I–*Xho* I fragment from the plasmids was then subcloned into pJR-FLΔSX that was created by replacing the *Stu* I–*Xho* I fragment of pJR-FL with a linker. The end products were proviral plasmids that were used for transfection for virus production. The procedure described above was repeated for construction of the proviral DNA containing two to four mutations.

For virus preparation, 293T cells (2×10^6) were transfected with 10 μg of proviral DNA using the calcium phosphate ProFection Mammalian Transfection System (Promega). The supernatant was collected 28 h after transfection, filtered through a 0.22-μm filter (Millipore), and stored at −80°C until further use. The amount of p24 Gag in the supernatant was measured by p24 Gag ELISA (Zeptometrix).

Viral replication assay

For the viral replication assay, 4×10^4 PM1/CCR5 cells were infected with 8 ng p24 Gag for 2 h in the presence or absence of 1 μM maraviroc. After washing twice with phosphate-buffered saline (PBS), the infected cells were incubated at 37°C in a 5% CO_2 atmosphere in the presence or absence of 1 μM maraviroc. On day 6 after infection, the amount of p24 Gag in the supernatant was measured by p24 Gag ELISA (Zeptometrix). Maraviroc was provided by the NIH AIDS Research and Reference Reagent Program, Division of AIDS National Institute of Allergy and Infectious Diseases.

Determination of drug susceptibility

Drug susceptibilities were determined by the single-round viral entry assay using previously titrated pseudotyped virus preparations with MAGIC-5 cells. In brief, MAGIC-5 cells were plated in 48-well tissue culture plates 1 day before infection. After absorption of the pseudotyped virus for 2 h at 37°C in the presence or absence of 1 μM maraviroc, the cells were washed twice with PBS and further incubated for 48 h in fresh medium in the presence or absence of the inhibitor.

HIV-1 single-cycle luciferase reporter assay

HIV-1 single-cycle luciferase reporter viruses were produced by cotransfection of 293T cells with pNL–LucR–E^- [33] and Env-expressing plasmids pCXN–EnvJR-FLan, pCXN–Env_{V3-M5}, pCXN–Env_{2345}, pCXN–Env_{1345}, pCXN–Env_{1245}, pCXN–Env_{1235}, or pCXN–Env_{1234}. Culture supernatant containing pseudoviruses at a final concentration of 1 ng/ml p24 was added to 1×10^4 cells/well MAGIC5 cells [28] in a 48-well plate. After 2 h, the cells were washed twice with phosphate-buffered saline (PBS) and firefly luciferase activity was measured 48 h postinfection, according to the manufacturer's directions (Promega).

Results

Noncompetitive-resistant virus HIV-1_{V3-M5}

HIV-1_{V3-M5} containing the five mutations I304V/F312W/T314A/E317D/I318V in the V3 loop with a JR-FL background (Figure 1A) exhibits noncompetitive resistance to maraviroc [15]. This virus could replicate in the presence of an extremely high concentration of the entry inhibitor (Figure 1B), i.e., 1 μM maraviroc, which was 147-fold higher than the IC_{50} value of the wild-type HIV-$1_{JR-FLan}$ (0.0069 μM). HIV-1_{V3-M5} could infect

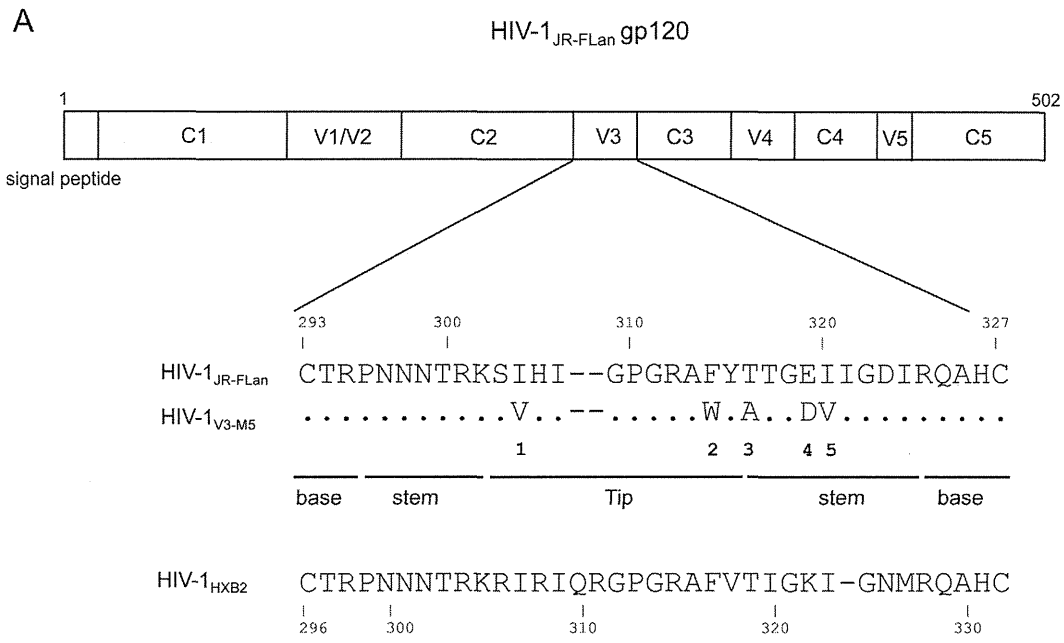

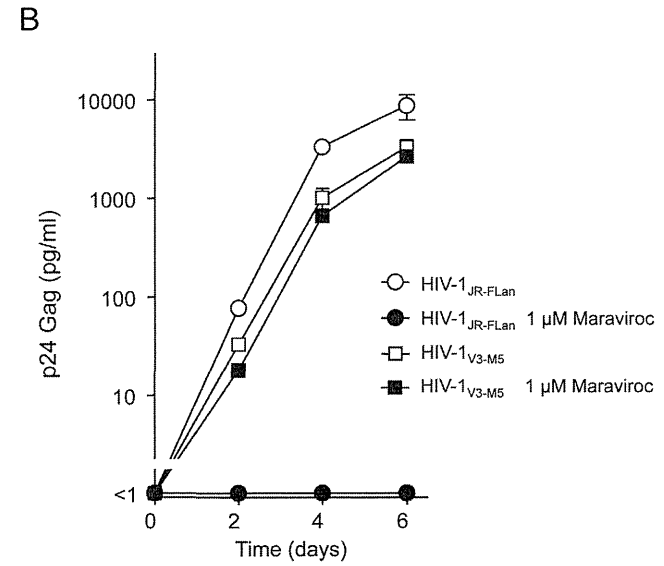

Figure 1. Noncompetitive resistant HIV-$1_{V3\text{-}M5}$. (A) Five amino acid substitutions in the V3 loop of HIV-$1_{V3\text{-}M5}$ (I304V/F312W/T314A/E317D/I318V). HIV-$1_{JR\text{-}FLan}$ was created form HIV-$1_{JR\text{-}FL}$ by incorporation of AflII and NheI. Incorporation of the NheI site led to amino acid substitutions Val^{342}-Ile^{343} to Ala^{342}-Ser^{343}. HIV-$1_{JR\text{-}FLan}$ was used as the parental virus. (B) Replication kinetics of HIV-$1_{V3\text{-}M5}$ in the presence or absence of 1 μM maraviroc in PM1/CCR5 cells. PM1/CCR5 cells (1×10^5) were infected with 10 ng of p24 Gag for 3 h. Viral replication was monitored by measuring p24 Gag in the supernatant after infection. The analysis was repeated three times; the error bars represent the S.D. of three replicates from one representative experiment.
doi:10.1371/journal.pone.0065115.g001

PM1/CCR5 cells through drug-bound CCR5 to produce p24 Gag in the presence or absence of 1 μM maraviroc, whereas HIV-$1_{JR\text{-}FLan}$ replication was completely suppressed.

Suppression of replication in recombinant viruses containing one to three mutations in the V3 loop by maraviroc

To further examine the contribution of each mutation to noncompetitive resistance, we constructed recombinant viruses containing one of the five mutations in the V3 loop (Figure 2A). I304V, F312W, T314A, E317D, and I318V were the polymorphic mutations detected in R5 clinical isolates. Thus, none of these viruses exhibited defective growth, although F312W caused a moderate decrease in p24 Gag production in the absence of maraviroc. HIV-$1_{V3\text{-}M5}$ replication was 1.8-fold lower than HIV-$1_{JR\text{-}FLan}$ replication. The presence of 1 μM maraviroc completely suppressed the production of recombinant viruses containing a single mutation, indicating that these single mutations could not confer noncompetitive resistance. Following this, we constructed 11 recombinant viruses, each containing two or three random combinations of the mutations (Figure 2B). Theoretically, the total

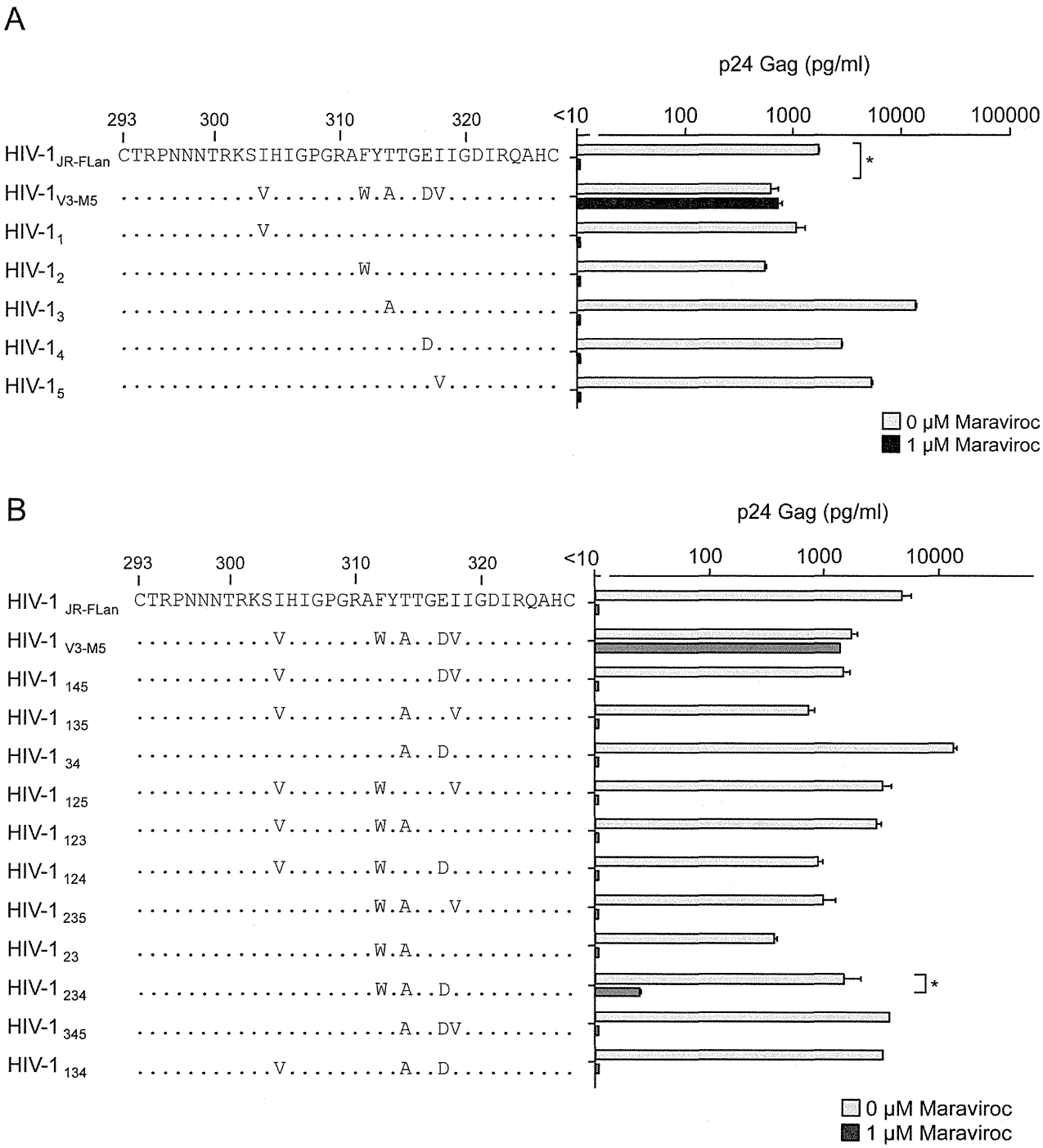

Figure 2. The effect of 1 μM of maraviroc on p24 Gag production in recombinant viruses containing one (A) and two or three (B) of the five amino acid substitutions. PM1/CCR5 cells (1×10^5) were infected with 10 ng p24 Gag for 3 h in the presence or absence of 1 μM maraviroc. On day 6 after infection, the amount of Gag in the supernatant was measured using HIV-1 p24 ELISA. The analysis was repeated three times; the error bars represent the S.D. of three replicates from one representative experiment. **, $p<0.01$. Statistical significant difference was calculated by *t* test.
doi:10.1371/journal.pone.0065115.g002

number of possible combinations of the five mutations was 120; therefore, 11 combinations of two or three mutations were insufficient to determine the crucial combination(s) for noncompetitive resistance. These recombinants could produce more than 100 pg/ml p24 Gag in the absence of maraviroc, although their replication resulted in variable levels of p24 Gag. Maraviroc mostly suppressed the replication of these recombinant viruses, indicating that the combination of these two or three mutations did not confer use of drug-bound CCR5 as a coreceptor for viral entry. However HIV-1_{234} containing F312W/T314A/E317D could replicate in the presence of 1 μM maraviroc, although p24 Gag production was 1.8% of that in its absence. We could not

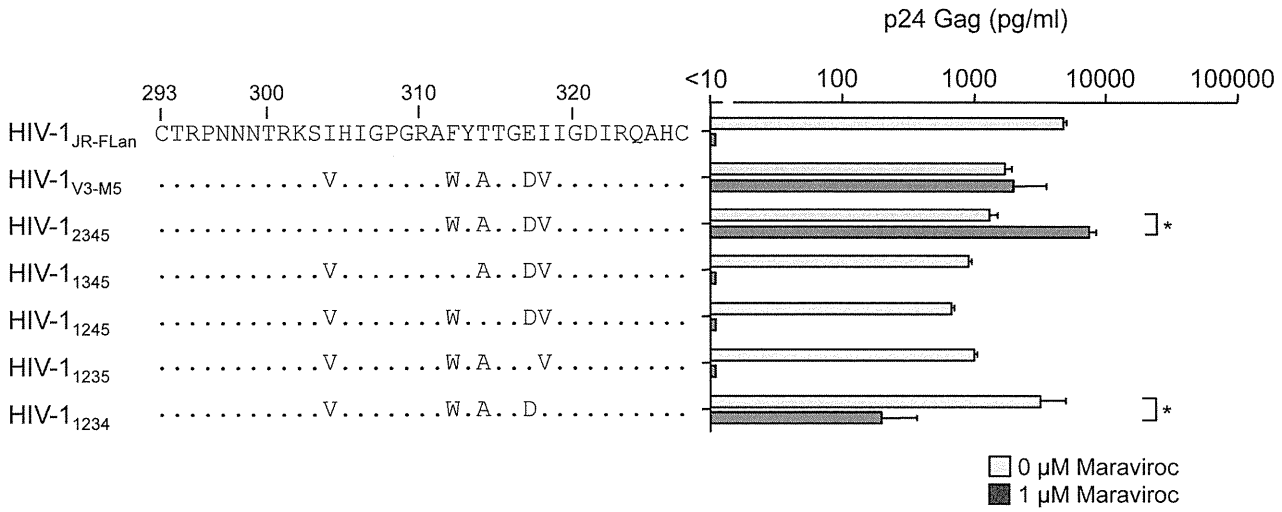

Figure 3. The effect of 1 μM of maraviroc on p24 Gag production in recombinant viruses containing four of the five amino acid substitutions. PM1/CCR5 cells (1×10^5) were infected with 10 ng p24 Gag for 3 h in the presence or absence of 1 μM maraviroc. On day 6 after infection, the amount of Gag in the supernatant was measured using HIV-1 p24 ELISA. The analysis was repeated three times; the error bars represent the S.D. of three replicates from one representative experiment. **, $p<0.01$. Statistical significant difference was calculated by *t* test.
doi:10.1371/journal.pone.0065115.g003

passage HIV-1_{234} in PM1/CCR5 cells because of its poor replication in the presence of 1 μM maraviroc (data not shown). These results suggest that HIV-1_{234} is an intermediate form in the transition of the wild type to a completely noncompetitive-resistant form.

Effect of maraviroc on recombinant viruses containing four mutations in the V3 loop

We next examined the recombinant viruses containing four mutations in the V3 loop (Figure 3). Without maraviroc, the viral fitness of HIV-1_{1234} was comparable with that of HIV-$1_{JR\text{-}FLan}$, whereas the other four recombinant viruses replicated at levels lower than those of HIV-$1_{V3\text{-}M5}$. Of note, HIV-1_{2345} and HIV-1_{1234} could replicate in the presence of 1 μM maraviroc, although HIV-1_{1345}, HIV-1_{1245}, and HIV-1_{1235} replication was completely suppressed. p24 Gag production by HIV-1_{2345} in the presence of maraviroc was 4.5-fold higher than that in its absence, whereas HIV-1_{1234} replication in the presence of maraviroc was 15-fold lower than that in the absence of maraviroc. These two viruses contained three common mutations: F312W, T314A, and E317D.

Effect of maraviroc on recombinant virus containing F312W/T314A/E317D in the V3 loop

We further examined whether HIV-1_{234} containing the triplet mutation F312W/T314A/E317D exhibited noncompetitive resistance (Figure 4). HIV-$1_{V3\text{-}M5}$ replication can be enhanced by T199K in V3 mutants to a level comparable with that in HIV-$1_{JR\text{-}FL}$ [15]. p24 Gag production by HIV-$1_{V3\text{-}M5/T199K}$ increased from 3100 pg/ml to 10,500 pg/ml in the presence of 1 μM maraviroc, whereas there was no significant increase in its absence. Similarly, HIV-$1_{234/T199K}$ replication was significantly enhanced from 31 pg/ml to 650 pg/ml in the presence of 1 μM maraviroc but not in its absence. These results indicated that triplet mutations in the V3 loop are crucial for noncompetitive resistance, and I304V, I318V, or T199K can increase viral fitness.

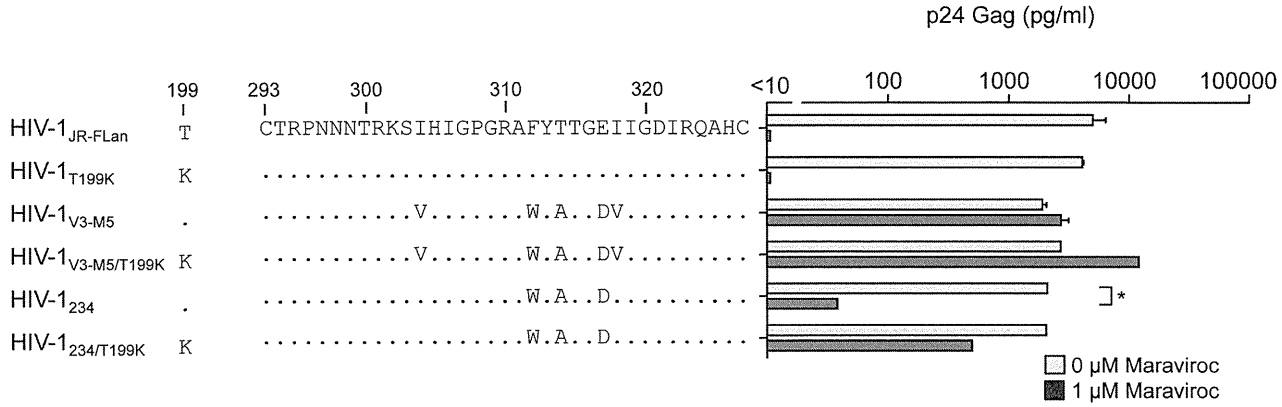

Figure 4. The effect of 1 μM of maraviroc on p24 Gag production in HIV-$1_{JR\text{-}FLan}$, HIV-1_{T199K}, HIV-$1_{V3\text{-}M5}$, HIV-$1_{V3\text{-}M5/T199K}$, HIV-1_{234}, and HIV-$1_{234/T199K}$. PM1/CCR5 cells (1×10^5) were infected with 10 ng p24 Gag for 3 h in the presence or absence of 1 μM maraviroc. On day 6 after infection, the amount of Gag in the supernatant was measured using HIV-1 p24 ELISA. The analysis was repeated three times; the error bars represent the S.D. of three replicates from one representative experiment. **, $p<0.01$. Statistical significant difference was calculated by *t* test.
doi:10.1371/journal.pone.0065115.g004

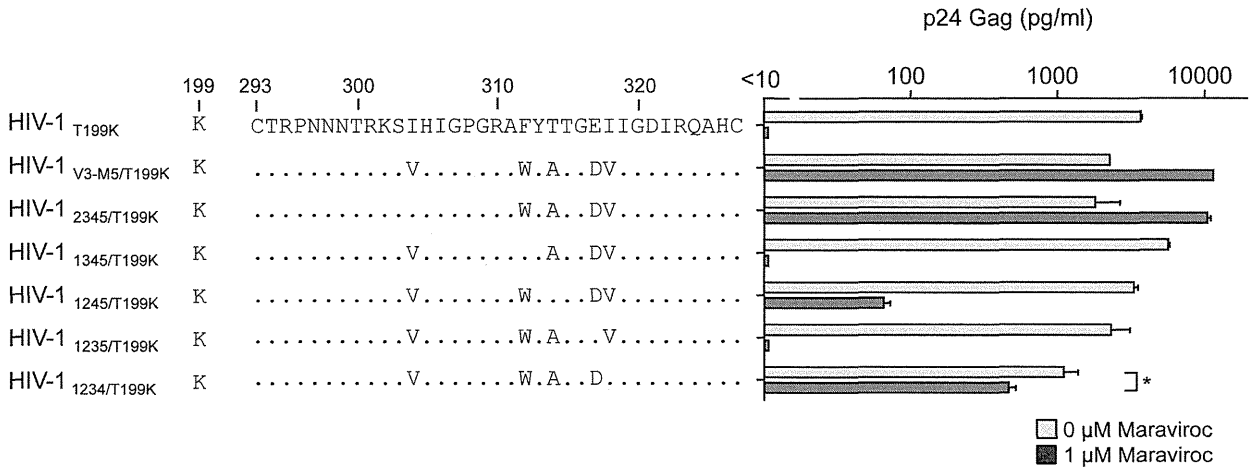

Figure 5. The effect of 1 μM of maraviroc on p24 Gag production in recombinant viruses containing four amino acid substitutions plus T199K. PM1/CCR5 cells (1×10^5) were infected with 10 ng p24 Gag for 3 h in the presence or absence of 1 μM maraviroc. On day 6 after infection, the amount of Gag in the supernatant was measured by HIV-1 p24 ELISA. The analysis was repeated three times; the error bars represent the S.D. of three replicates from one representative experiment. *, $p<0.05$; **, $p<0.01$. Statistical significant difference was calculated by *t* test.
doi:10.1371/journal.pone.0065115.g005

Finally, we examined the effects of T199K on the replication of recombinant viruses carrying four mutations in the V3 loop. In the presence of maraviroc, HIV-1_{1234} produced 6.7% of p24 Gag of that in its absence (Figure 3); however, HIV-$1_{1234/T199K}$ replication increased up to 43% (Figure 5). Of note, HIV-1_{1245} replication was completely suppressed by 1 μM maraviroc (Figure 3); however, HIV-$1_{1245/T199K}$ could replicate in the presence of 1 μM maraviroc, although the p24 production was only 2% of that in the absence maraviroc (Figure 5). These results indicated that the absence of T314A in the triplet could be compensated by I304V, I318V, or T199K and result in noncompetitive resistance.

Susceptibilities of pseudotyped viruses containing four mutations in the V3 loop to maraviroc

To confirm the phenotypes of the recombinant viruses determined by the single-round infection assay using MAGIC-5 cells, we examined the susceptibility of viral entry using pseudotyped viruses with mutant envelopes (Figure 6). The viral entry of HIV-$1_{JR\text{-}FLan}$ Env, HIV-1_{1345} Env, or HIV-1_{1235} Env was completely suppressed by maraviroc. These results were consistent with those obtained using competent viruses (Figure 3). HIV-$1_{V3\text{-}M5}$ Env inhibition with maraviroc saturated approximately 17% entry efficiency [15]. HIV-1_{1234} Env retained 4% entry efficiency in the presence of 1 μM maraviroc, indicating that the low efficiency of drug-bound CCR5 usage accounted for the low replication rate of the competent virus. In contrast, HIV-1_{2345} Env could infect MAGIC-5 cells with 41% entry efficiency of that in the absence of maraviroc (Figure 6), although viral fitness in the presence of the inhibitor was superior to that in its absence in PM1/CCR5 cells (Figure 3). Furthermore, even 1 μM maraviroc did not completely suppress HIV-1_{1245} Env entry (Figure 6). These discrepancies may have occurred because of the cell-type-specific nature of noncompetitive resistance [34].

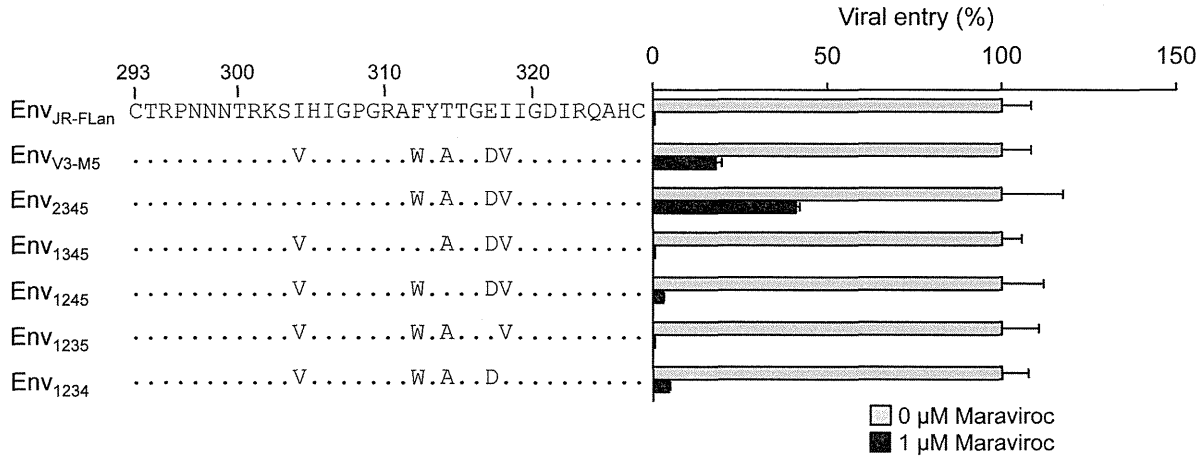

Figure 6. Maraviroc susceptibility of pseudotyped viruses derived from HIV-$1_{JR\text{-}FLan}$, HIV-$1_{V3\text{-}M5}$, HIV-1_{2345}, and HIV-1_{1345}, HIV-1_{1245}, HIV-1_{1235}, and HIV-1_{1234}. MAGIC-5 cells were infected with pseudotyped viruses in the absence or presence of 1 μM maraviroc. The analysis was repeated three times; the error bars represent the S.D. of three replicates from one representative experiment. **, $p<0.01$. Statistical significant difference was calculated by *t* test.
doi:10.1371/journal.pone.0065115.g006

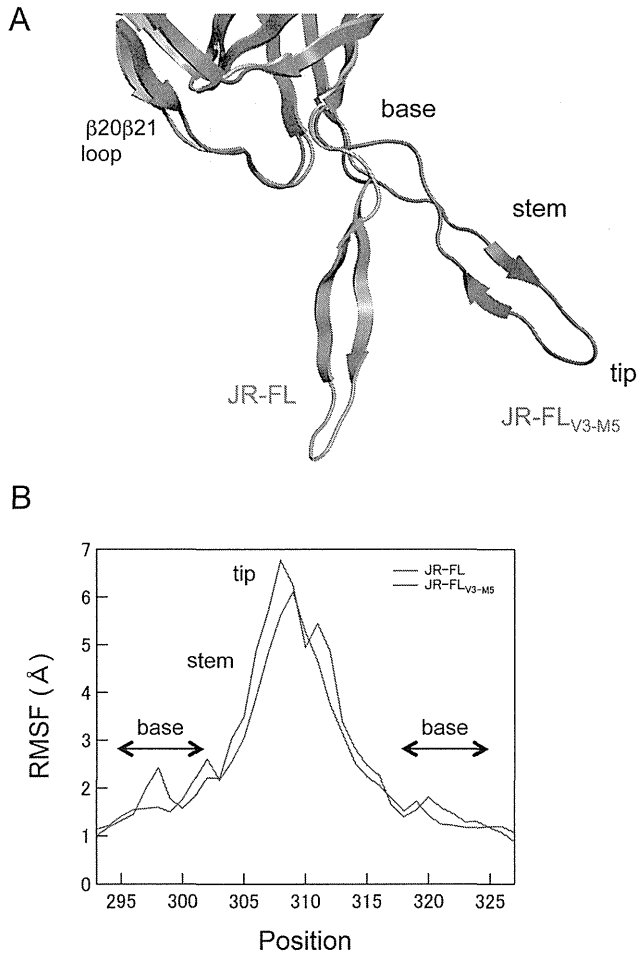

Figure 7. MD simulation of the HIV-1 gp120 outer domain. (A) Superimposition of averaged structures obtained from 40,000 snapshots during the 10–20 ns of MD simulation. Grey and blue ribbons indicate the gp120 V3 of JR-FL$_{an}$ and JR-FL$_{V3-M5}$, respectively. (B) Distribution of RMSF in the V3 region of gp120. The RMSF values indicate the atomic fluctuations of the main chains of individual amino acids during the 10–20 ns of MD simulations.
doi:10.1371/journal.pone.0065115.g007

MD simulations of the HIV-1 gp120 outer domain

MD simulation is a powerful computational method for studying motions of proteins at the atomic-scale [23–25]. To address structural impacts of the V3 maraviroc-resistance mutations, we performed MD simulations of the HIV-1$_{JR-FL}$ gp120 outer domain V3 loop with and without the five mutations of HIV-1$_{V3-M5}$ (I304V/F312W/T314A/E317D/I318V). As described previously [21,22], the root mean square deviation (RMSD) between the initial model and the model at a given time of MD simulation sharply increased soon after heating the initial model and then fluctuated continually for 20 ns of simulations (data not shown). The data suggests an intrinsic property of the gp120 outer domain V3 loops that results in structural fluctuations in solution. Hence, we constructed averaged gp120 structures using 40,000 snapshots during the 10–20 ns of MD simulation, and we superimposed them to reveal structural differences in the V3 loops of the two gp120s. Marked changes in V3 conformation were induced by introduction of the five V3 mutations (Figure 7A). The V3 loop of JR-FL$_{V3-M5}$ was located at a much more distant position from the β20β21 loop in the outer domain than that of JR-FL. In addition, an anti-parallel β-sheet in the V3 stem region was reduced in the V3 loop of JR-FL$_{V3-M5}$ compared with that of JR-FL.

To map the V3 loop sites in which fluctuations are influenced by the five mutations, we calculated the root mean square fluctuation (RMSF) of the main chains of individual amino acids in the V3 loop using 40,000 snapshots from 10–20 ns of each MD simulation (Figure 7B). The RMSF values were maximal at the V3 tip, indicating that the region involved in binding to CCR5 ECL2 fluctuates the most in solution. Interestingly, the five mutations were found to decrease the RMSF throughout the V3 tip and stem regions (Figure 7B, blue line). In addition, the five mutations caused a shift in small RMSF peaks at V3 base regions.

Discussion

In this study, we examined the genetic and structural bases for the noncompetitive resistance of HIV-1 to maraviroc. Using site-directed mutagenesis, we demonstrated that combinations of mutations in V3 are required to confer maraviroc resistance to the HIV-1$_{JR-FL}$ strain (Figures 2, 3). In addition, we showed that in combination with the V3 mutations, a T199K mutation in the C2 region enhanced viral fitness (Figures 4, 5). Finally, we indicated that these five maraviroc-resistance V3 mutations of HIV-1$_{V3-M5}$ change the intrinsic structures and motion of the V3 loop on the HIV-1 gp120 outer domain. These data provide novel insights into the molecular mechanisms of HIV-1 maraviroc resistance. Further study may be able to classify the structure of V3 loop of HIV-1 to reveal or easily develop noncompetitive resistance through antiviral treatment with maraviroc in advance.

In the V3 loop, maraviroc-associated mutations have been reported at His^{305}, Pro^{308}, Ala^{311}, Phe^{312}, Thr^{314}, Glu^{317}, and Ile^{318} (numbering in JR-FL) [11,35–37]. In the HIV-1$_{JR-FLan}$ background, F312W/T314A/E317D is a crucial combination for maraviroc resistance, and I318V was required for extensive replication comparable with that in the wild type (Figure 5). HIV-1$_{234}$ could not be passaged in PM1/CCR5 cells in the presence of 1 μM maraviroc because of its poor viral fitness (data not shown), suggesting that F312W/T314A/E317D is a type of fitness "valley" that needs to be selected on the genetic pathway for the development of noncompetitive resistance. F312W/T314A/E317D and one other mutation are required to acquire noncompetitive resistance. We could not select a maraviroc-resistant virus from the homogeneous viral population of HIV-1$_{JR-FLan}$ because spontaneous multiple mutations ($\geq$4) were unlikely to occur during *in vitro* passages, whereas our V3 virus library inherently contained F312W/T314A/E317D and fitness-enhancing mutations (I304V/I318V) [15]. We could not observe the condensation of viral clones containing one or two of these mutations at low concentrations of maraviroc (0.03–0.1 μM), suggesting that one or two combinations of these mutations did not confer a selective advantage (Figure 2). HIV-1 did not acquire maraviroc resistance by following a pathway for increasing resistance by the accumulation of multiple mutations. Instead, spontaneous alterations in the V3 loop were required to utilize maraviroc-bound CCR5. These results suggest that a virus library containing various mutations in specific regions such as the V3 loop is suitable for the *in vitro* selection of viruses resistant to entry inhibitors [38].

It remains unclear how the maraviroc resistant viruses use maraviroc-bound CCR5 as an entry coreceptor. Accumulating evidence from the investigations of protein chemistry indicates that structural fluctuations of the protein surface in solution play key roles in these molecular interactions [23–25]. Therefore, it is possible that the resistant viruses adjust these structural fluctua-

tions of coreceptor binding surfaces through V3 mutations that enable binding to maraviroc-bound CCR5. In general, it is difficult to analyze motions of proteins at an atomic scale. However, recent advances in hardware and software of biomolecular simulation have rapidly improved its precision and performance [23–25]. Therefore, in this study we applied MD simulations and elucidated the structural dynamics of the gp120 outer domain in solution.

Our MD simulations of the gp120 outer domain suggest that the five mutations in the V3 loop of HIV-$1_{V3\text{-}M5}$ caused marked changes in the physical properties of the CCR5 binding surface (Figure 7). Firstly, the mutations altered configurations and secondary structure of the tip-stem region of V3 loop on gp120. Secondly, the mutations reduced fluctuations at the base and tip regions of the V3 loop on gp120 and shifted the site of these fluctuations to the V3 base region. These results illustrate how maraviroc-resistance mutations have an impact on the intrinsic properties and structural motions of the V3 loops on the HIV-1 gp120 outer domain at the atomic-level. The altered configuration and/or fluctuation of the mutant V3 loops may advantageously support binding to drug-bound CCR5 by attenuating fluctuations on its surface. Further MD simulations in combination with experiments will clarify which of these structural changes are critical for the maraviroc resistance of HIV-1.

Author Contributions

Conceived and designed the experiments: YY KY. Performed the experiments: YY MY YM HT SH. Analyzed the data: YY MY YM SH HS KY. Contributed reagents/materials/analysis tools: YY MY YM SH HS KY. Wrote the paper: YY HS KY.

References

1. Tilton JC, Wilen CB, Didigu CA, Sinha R, Harrison JE, et al. (2010) A maraviroc-resistant HIV-1 with narrow cross-resistance to other CCR5 antagonists depends on both N-terminal and extracellular loop domains of drug-bound CCR5. J Virol 84: 10863–10876.
2. Fadel H, Temesgen Z (2007) Maraviroc. Drugs Today (Barc) 43: 749–758.
3. Tilton JC, Doms RW (2010) Entry inhibitors in the treatment of HIV-1 infection. Antiviral Res 85: 91–100.
4. Gorry PR, Ancuta P (2011) Coreceptors and HIV-1 pathogenesis. Curr HIV/AIDS Rep 8: 45–53.
5. Gulick RM, Su Z, Flexner C, Hughes MD, Skolnik PR, et al. (2007) Phase 2 study of the safety and efficacy of vicriviroc, a CCR5 inhibitor, in HIV-1-Infected, treatment-experienced patients: AIDS clinical trials group 5211. J Infect Dis 196: 304–312.
6. Moore JP, Kuritzkes DR (2009) A piece de resistance: how HIV-1 escapes small molecule CCR5 inhibitors. Curr Opin HIV AIDS 4: 118–124.
7. Westby M, van der Ryst E (2010) CCR5 antagonists: host-targeted antiviral agents for the treatment of HIV infection, 4 years on. Antivir Chem Chemother 20: 179–192.
8. Kuhmann SE, Pugach P, Kunstman KJ, Taylor J, Stanfield RL, et al. (2004) Genetic and phenotypic analyses of human immunodeficiency virus type 1 escape from a small-molecule CCR5 inhibitor. J Virol 78: 2790–2807.
9. Trkola A, Kuhmann SE, Strizki JM, Maxwell E, Ketas T, et al. (2002) HIV-1 escape from a small molecule, CCR5-specific entry inhibitor does not involve CXCR4 use. Proc Natl Acad Sci U S A 99: 395–400.
10. Marozsan AJ, Kuhmann SE, Morgan T, Herrera C, Rivera-Troche E, et al. (2005) Generation and properties of a human immunodeficiency virus type 1 isolate resistant to the small molecule CCR5 inhibitor, SCH-417690 (SCH-D). Virology 338: 182–199.
11. Westby M, Smith-Burchnell C, Mori J, Lewis M, Mosley M, et al. (2007) Reduced maximal inhibition in phenotypic susceptibility assays indicates that viral strains resistant to the CCR5 antagonist maraviroc utilize inhibitor-bound receptor for entry. J Virol 81: 2359–2371.
12. Pugach P, Marozsan AJ, Ketas TJ, Landes EL, Moore JP, et al. (2007) HIV-1 clones resistant to a small molecule CCR5 inhibitor use the inhibitor-bound form of CCR5 for entry. Virology 361: 212–228.
13. Baba M, Miyake H, Wang X, Okamoto M, Takashima K (2007) Isolation and characterization of human immunodeficiency virus type 1 resistant to the small-molecule CCR5 antagonist TAK-652. Antimicrob Agents Chemother 51: 707–715.
14. Ogert RA, Wojcik L, Buontempo C, Ba L, Buontempo P, et al. (2008) Mapping resistance to the CCR5 co-receptor antagonist vicriviroc using heterologous chimeric HIV-1 envelope genes reveals key determinants in the C2-V5 domain of gp120. Virology 373: 387–399.
15. Yuan Y, Maeda Y, Terasawa H, Monde K, Harada S, et al. (2011) A combination of polymorphic mutations in V3 loop of HIV-1 gp120 can confer noncompetitive resistance to maraviroc. Virology 413: 293–299.
16. Rizzuto CD, Wyatt R, Hernandez-Ramos N, Sun Y, Kwong PD, et al. (1998) A conserved HIV gp120 glycoprotein structure involved in chemokine receptor binding. Science 280: 1949–1953.
17. Rizzuto C, Sodroski J (2000) Fine definition of a conserved CCR5-binding region on the human immunodeficiency virus type 1 glycoprotein 120. AIDS Res Hum Retroviruses 16: 741–749.
18. Cormier EG, Dragic T (2002) The crown and stem of the V3 loop play distinct roles in human immunodeficiency virus type 1 envelope glycoprotein interactions with the CCR5 coreceptor. J Virol 76: 8953–8957.
19. Cormier EG, Tran DN, Yukhayeva L, Olson WC, Dragic T (2001) Mapping the determinants of the CCR5 amino-terminal sulfopeptide interaction with soluble human immunodeficiency virus type 1 gp120-CD4 complexes. J Virol 75: 5541–5549.
20. Thorpe IF, Brooks CL 3rd (2007) Molecular evolution of affinity and flexibility in the immune system. Proc Natl Acad Sci U S A 104: 8821–8826.
21. Yokoyama M, Naganawa S, Yoshimura K, Matsushita S, Sato H (2012) Structural dynamics of HIV-1 envelope Gp120 outer domain with V3 loop. PLoS One 7: e37530.
22. Naganawa S, Yokoyama M, Shiino T, Suzuki T, Ishigatsubo Y, et al. (2008) Net positive charge of HIV-1 CRF01_AE V3 sequence regulates viral sensitivity to humoral immunity. PLoS One 3: e3206.
23. Ode H, Nakashima M, Kitamura S, Sugiura W, Sato H (2012) Molecular dynamics simulation in virus research. Front Microbiol 3: 258.
24. Karplus M, Kuriyan J (2005) Molecular dynamics and protein function. Proc Natl Acad Sci U S A 102: 6679–6685.
25. Dodson GG, Lane DP, Verma CS (2008) Molecular simulations of protein dynamics: new windows on mechanisms in biology. EMBO Rep 9: 144–150.
26. Lusso P, Earl PL, Sironi F, Santoro F, Ripamonti C, et al. (2005) Cryptic nature of a conserved, CD4-inducible V3 loop neutralization epitope in the native envelope glycoprotein oligomer of CCR5-restricted, but not CXCR4-using, primary human immunodeficiency virus type 1 strains. J Virol 79: 6957–6968.
27. Maeda Y, Foda M, Matsushita S, Harada S (2000) Involvement of both the V2 and V3 regions of the CCR5-tropic human immunodeficiency virus type 1 envelope in reduced sensitivity to macrophage inflammatory protein 1alpha. J Virol 74: 1787–1793.
28. Hachiya A, Aizawa-Matsuoka S, Tanaka M, Takahashi Y, Ida S, et al. (2001) Rapid and simple phenotypic assay for drug susceptibility of human immunodeficiency virus type 1 using CCR5-expressing HeLa/CD4(+) cell clone 1–10 (MAGIC-5). Antimicrob Agents Chemother 45: 495–501.
29. Huang CC, Tang M, Zhang MY, Majeed S, Montabana E, et al. (2005) Structure of a V3-containing HIV-1 gp120 core. Science 310: 1025–1028.
30. Case DA, TAD, Cheatham III TE, Simmerling CL, Wang JM, et al. (2006) AMBER 9. San Francisco: University of California.
31. Hornak V, Abel R, Okur A, Strockbine B, Roitberg A, et al. (2006) Comparison of multiple Amber force fields and development of improved protein backbone parameters. Proteins 65: 712–725.
32. Jorgensen WL, Chandrasekhar J, Madura JD, Impey RW, Klein ML (1983) Comparison of simple potential functions for simulating liquid water. J Chem Phys 79: 926–935.
33. Mariani R, Rutter G, Harris ME, Hope TJ, Krausslich HG, et al. (2000) A block to human immunodeficiency virus type 1 assembly in murine cells. J Virol 74: 3859–3870.
34. Roche M, Jakobsen MR, Sterjovski J, Ellett A, Posta F, et al. (2011) HIV-1 escape from the CCR5 antagonist maraviroc associated with an altered and less-efficient mechanism of gp120-CCR5 engagement that attenuates macrophage tropism. J Virol 85: 4330–4342.
35. Tilton JC, Amrine-Madsen H, Miamidian JL, Kitrinos KM, Pfaff J, et al. (2010) HIV type 1 from a patient with baseline resistance to CCR5 antagonists uses drug-bound receptor for entry. AIDS Res Hum Retroviruses 26: 13–24.
36. Maeda Y, Yoshimura K, Miyamoto F, Kodama E, Harada S, et al. (2011) In vitro and In vivo Resistance to Human Immunodeficiency Virus Type 1 Entry Inhibitors. AIDS Clin Res.
37. Berro R, Klasse PJ, Jakobsen MR, Gorry PR, Moore JP, et al. (2012) V3 determinants of HIV-1 escape from the CCR5 inhibitors Maraviroc and Vicriviroc. Virology 427: 158–165.
38. Yusa K, Maeda Y, Fujioka A, Monde K, Harada S (2005) Isolation of TAK-779-resistant HIV-1 from an R5 HIV-1 GP120 V3 loop library. J Biol Chem 280: 30083–30090.

Citation: Molecular Therapy—Nucleic Acids (2013) 2, e137; doi:10.1038/mtna.2013.64

www.nature.com/mtna

Promoter Targeting shRNA Suppresses HIV-1 Infection *In vivo* Through Transcriptional Gene Silencing

Kazuo Suzuki[1], Shinichiro Hattori[2], Katherine Marks[1], Chantelle Ahlenstiel[3], Yosuke Maeda[4], Takaomi Ishida[5], Michelle Millington[6], Maureen Boyd[6], Geoff Symonds[1,6], David A Cooper[1,3], Seiji Okada[2] and Anthony D Kelleher[1,3]

Despite prolonged and intensive application, combined antiretroviral therapy cannot eradicate human immunodeficiency virus (HIV)-1 because it is harbored as a latent infection, surviving for long periods of time. Alternative approaches are required to overcome the limitations of current therapy. We have been developing a short interfering RNA (siRNA) gene silencing approach. Certain siRNAs targeting promoter regions of genes induce transcriptional gene silencing. We previously reported substantial transcriptional gene silencing of HIV-1 replication by an siRNA targeting the HIV-1 promoter *in vitro*. In this study, we show that this siRNA, expressed as a short hairpin RNA (shRNA) (shPromA-JRFL) delivered by lentiviral transduction of human peripheral blood mononuclear cells (PBMCs), which are then used to reconstitute NOJ mice, is able to inhibit HIV-1 replication *in vivo*, whereas a three-base mismatched variant (shPromA-M2) does not. In shPromA-JRFL–treated mice, HIV-1 RNA in serum is significantly reduced, and the ratio of CD4$^+$/CD8$^+$ T cells is significantly elevated. Expression levels of the antisense RNA strand inversely correlates with HIV-1 RNA in serum. The silenced HIV-1 can be reactivated by T-cell activation in *ex vivo* cultures. HIV-1 suppression is not due to offtarget effects of shPromA-JRFL. These data provide "proof-of principle" that an shRNA targeting the HIV-1 promoter is able to suppress HIV-1 replication *in vivo*.

Molecular Therapy—Nucleic Acids (2013) **2**, e137; doi:10.1038/mtna.2013.64; published online 3 December 2013
Subject Category: siRNAs, shRNAs, and miRNAs Therapeutic proof-of-concept

Introduction

Currently available combined antiretroviral therapy has markedly improved both morbidity and mortality associated with human immunodeficincy cirus (HIV)-1 infection, reducing the viral load ((VL) HIV-1 RNA in serum) and rescuing CD4$^+$ T cells from HIV-1 infection.[1–4] However, HIV-1 persists in its proviral form in cellular reservoirs.[5–7] On cessation of even prolonged combined antiretroviral therapy, rapid viral recrudescence occurs in the overwhelming majority of cases.[8,9] Alternative therapeutic approaches are required to overcome these limitations. We have been investigating a transcriptional gene silencing (TGS) approach using short interfering RNAs (siRNAs) gene targeting the promoter region of HIV-1. Unlike siRNA targeting HIV-1 messenger RNA (mRNA), which induces the post-TGS (PTGS) pathway to degrade mRNA in the cytoplasm, we and others have shown that specific siRNAs targeting viral promoter regions can induce TGS within the nucleus.[10–16] TGS has also been demonstrated in an *in vivo* model targeting the promoter of vascular endothelial growth factor (VEGF-A).[17]

Although initial reports demonstrated inhibition of HIV-1 replication by siRNA through PTGS,[18,19] further *in vitro* studies revealed a number of modes of resistance: directly, through rapid development of mutations within[20–22] or near the siRNA targeted region,[23] and indirectly, via mutations in regions separate from the RNA interference targets.[24] Nonetheless, both direct and indirect modes of resistance compromise the efficacy of combinations of siRNAs targeting multiple HIV mRNA regions.[25] Therefore, PTGS approaches appear to have fundamental limitations.

siRNA-induced TGS was originally reported in plants.[26–29] TGS has more recently been observed in certain mammalian cells.[11,30,31] TGS has potential advantages over PTGS when silencing of HIV is the objective. The high mutation rate of HIV-1, due to its nonproof reading reverse transcriptase (RT) and high replication rates, allows rapid adaptation to environmental pressures including the development of resistance or escape mutations.[32,33] As TGS results in marked reduction of HIV-1 transcription through induction of epigenetic modifications in the HIV-1 promoter,[34] production of new viral RNA is limited and the HIV-1 RT enzyme has no substrate on which to act. Therefore, resistance mutations are less likely to develop in a TGS approach.[16] However, TGS approaches may have their own pitfalls. Offtarget effects must be carefully excluded as they have been described with siRNAs or antisense RNA designed to induce TGS.[35] Sequence-specific offtarget effects are difficult to predict and even slight offsetting of target sequences can make substantial changes to the extent of offtarget effects.[36] Furthermore, sequence-nonspecific offtarget effects can be induced by the triggering of interferon (IFN) pathways by double-stranded RNA through endosomal receptors such as Toll-like receptor (TLR)3, TLR7, and TLR8.[37,38]

We have reported sustained, profound, highly specific viral suppression of viral replication by siRNA- and short heparin RNA (shRNA)–induced TGS of HIV-1 and simian immunodeficiency virus in various *in vitro* models, through a mechanism that results in chromatin compaction.[34,39–42] Because HIV-1 has identical long terminal repeats (LTRs) at the 5′ and 3′ ends of the integrated virus, any promoter-targeted siRNA

[1]St. Vincent's Centre for Applied Medical Research, Darlinghurst, New South Wales, Australia; [2]Center for AIDS Research, Kumamoto University, Kumamoto, Japan; [3]The Kirby Institute, The University of New South Wales, New South Wales, Australia; [4]Department of Medical Virology, Faculty of Life Sciences, Kumamoto University, Kumamoto, Japan; [5]Research Center for Asian Infectious Disease, Institute of Medical Science, University of Tokyo, Tokyo, Japan; [6]Calimmune, Sydney, Australia. Correspondence: Kazuo Suzuki, St. Vincent's Centre for Applied Medical Research Darlinghurst, New South Wales, Australia. E-mail: k.suzuki@amr.org.au
Received 21 August 2013; accepted 23 September 2013; advance online publication 3 December 2013. doi:10.1038/mtna.2013.64

can potentially act through PTGS. With our lead candidate, called PromA, we have found that the contribution of PTGS is limited.[34] In this study, we used a lentiviral delivery system to express the previously described shRNA targeting the HIV-1 promoter region to transduce human PBMCs. We first assessed shRNA-mediated TGS approach using a PBMC infection model *in vitro*. We then demonstrated an antiviral effect of this construct on HIV-1 infection *in vivo* using NOJ mice[43] transplanted with the lenivirus-transduced PBMCs.

Results

shRNA targeting the promoter of HIV-1_{JRFL} suppresses viral expression in PBMCs obtained from healthy donors

Our previous *in vitro* TGS studies were based on PromA targeting the NF-κβ region of the U3 promoter region of HIV-1 (**Figure 1a**). The humanized NOD/SCID Janus kinase 3 knockout mice model has been developed to use the HIV-1_{JRFL} strain.[43] We sequenced the HIV-1_{JRFL} promoter region, which demonstrated that there was a one-base mismatch compared with the original sequence targeted by PromA (**Figure 1a**). Because induction of TGS is sequence specific, and a two-base mismatched siRNA failed to induce effective TGS *in vitro*,[42] we constructed U6 promoter driven–shRNA expression self-inactivated lentivirus vector plasmids with a GFP expression unit (**Figure 1b**) specifically targeting this region of HIV_{JRFL} (shPromA-JRFL), as well as shPromA-M2, a three-base mismatched control, and shPromA-Sc (a scrambled control) (**Figure 1b**). VSV-G envelope pseudotype lentiviruses expressing each of these constructs were used to transduce human PBMCs. A transduction efficiency of 38.4% for shPromA-JRFL, 31.7% for shPromA-M2, and 34.7% for shPromA-Sc was achieved as assessed by EGFP expression 5 days after transduction (**Figure 1c**). PBMCs transduced with shPromA-JRFL, but not those transduced with control lentivirus, challenged with HIV-1 *in vitro*, showed significant reduction of HIV-1 *gag* mRNA (**Figure 1d**).

The detection of *gag* mRNA reflects transcription of unspliced viral RNA. We also investigated whether the transcription of spliced viral RNA was modulated by shPromA-JRFL by measuring levels of spliced-*tat* RNA (**Figure 1e**). As expected, shPromA-JRFL spliced-*tat* expression was significantly reduced, but with a different kinetic to the suppression of *gag* RNA. This results in a marked difference in the kinetics of the ratio of spliced (*tat*): unspliced (*gag*) RNA in the shPromA-JRFL–treated cultures compared with the control cultures with a peak in the spliced:unspliced ratio at day 7 (**Figure 1f**). By day 14, the levels of both *gag* and spliced-*tat* RNA are similar in each of the cultures, consistent with loss of effect. Sequence of the virus obtained from the culture supernatant of PBMCs transduced with lenti-shPromA-JRFL at day 14 did not show any mutations in U3 region and, in particular, in the shRNA target sequence. Given that only 38.4% of cells in these bulk cultures were transduced, these results suggest that the elevated HIV-1 replication by day 14, as assessed by both spliced and unspliced viral RNA, is likely due to overgrowth of virus from untransduced cells. Having demonstrated the *in vitro* efficacy of our new construct, we proceeded to *in vivo* experiments using shPromA-M2 as a control, because this three-base mismatched control is a more rigorous specificity control than the scrambled shPromA sequence.

shPromA-JRFL inhibits HIV-1 replication in a humanized NOJ mouse model

We evaluated the *in vivo* antiviral effect of shPromA-JRFL in a previously established model of acute HIV-1 infection based on the nonobese diabetic (NOD)/SCID/Janus kinase 3 knockout (NOJ) mice reconstituted with human PBMCs and then infected with HIV_{JRFL}.[43] First, we transduced healthy human PBMCs with lentivirus-expressing shPromA-JRFL or shPromA-M2. Transduction efficiency before transplantation was 22% for shPromA-JRFL and 25% for shPromA-M2. Seven days later, mice ($n = 8$ per group) were transplanted with 1×10^7 (nonselected) lentivirus-transduced PBMCs per-mouse by intraperitoneal injection and the cells allowed to engraft. Five days later, mice were infected by intraperitoneal inoculation of HIV-1_{JRFL} (**Figure 2a**). This is a model of rapidly progressive HIV-1 infection with high VLs, massive $CD4^+$ T-cell depletion, and profound immunodeficiency occurring within weeks of infection.[43]

Mononuclear cells were recovered at sacrifice (day 14 after HIV-1 infection) from the peritoneal cavity and the spleen. VL in serum was detected by RT quantitative real-time PCR (RT-qPCR). VL in the mice transplanted with PBMCs expressing shPromA-JRFL was significantly lower ($P = 0.014$) than in shPromA-M2 control mice (**Figure 2b**). $CD4^+$ T cells were reduced relative to $CD8^+$ T cells in shPromA-M2–transplanted mice, whereas the $CD4^+$ to $CD8^+$ T-cell ratio was better preserved in mice transplanted with shPromA-JRFL both in the peritoneal cavity ($P = 0.038$) and in the spleen ($P = 0.002$) (**Figure 2c**). Furthermore, the extent of downregulation of CD4 surface expression is reduced by shPromA-JRFL (**Supplementary Figure S1**). Thus, shPromA-JRFL appears to protect $CD4^+$ T cells against HIV-1–mediated depletion and downregulation of CD4 surface expression. By contrast, there was no significant difference in $CD8^+$ T-cell numbers between the two groups, indicating successful human PBMC engraftment in all the mice (**Supplementary Figure S2**). Intracellular staining after gating on human $CD3^+$ $CD8^-$ spleen cells demonstrated that the percentage of p24-expressing ($p24^+$) cells was significantly lower in the mice transplanted with shPromA-JRFL–transduced PBMCs ($P = 0.014$) (**Figure 2d**).

Expression levels of the antisense strand of shPromA-JRFL inversely correlated with VL

The above data indicate a reduction in viral replication and relative protection from $CD4^+$ T-cell destruction, but there was substantial variability in the extent of these effects among the mice within the PromA-JRFL–treated group. Previous observations have suggested that the antisense strand of double-stranded siRNA is responsible for induction of TGS in mammalian cells.[14,39,44] After transduction of the shPromA-JRFL lentivirus, the shRNA expression unit is transcribed from the U6 promoter, by RNA polymerase III, which terminates at a poly(T) motif within this expression unit. The short hairpin loop sequence is then processed by cellular ribonucleases to form mature/processed double-stranded siRNA.[45] We, therefore, quantified the antisense strand of the shPromA-JRFL transcript by real-time PCR, as previously described,[42] to

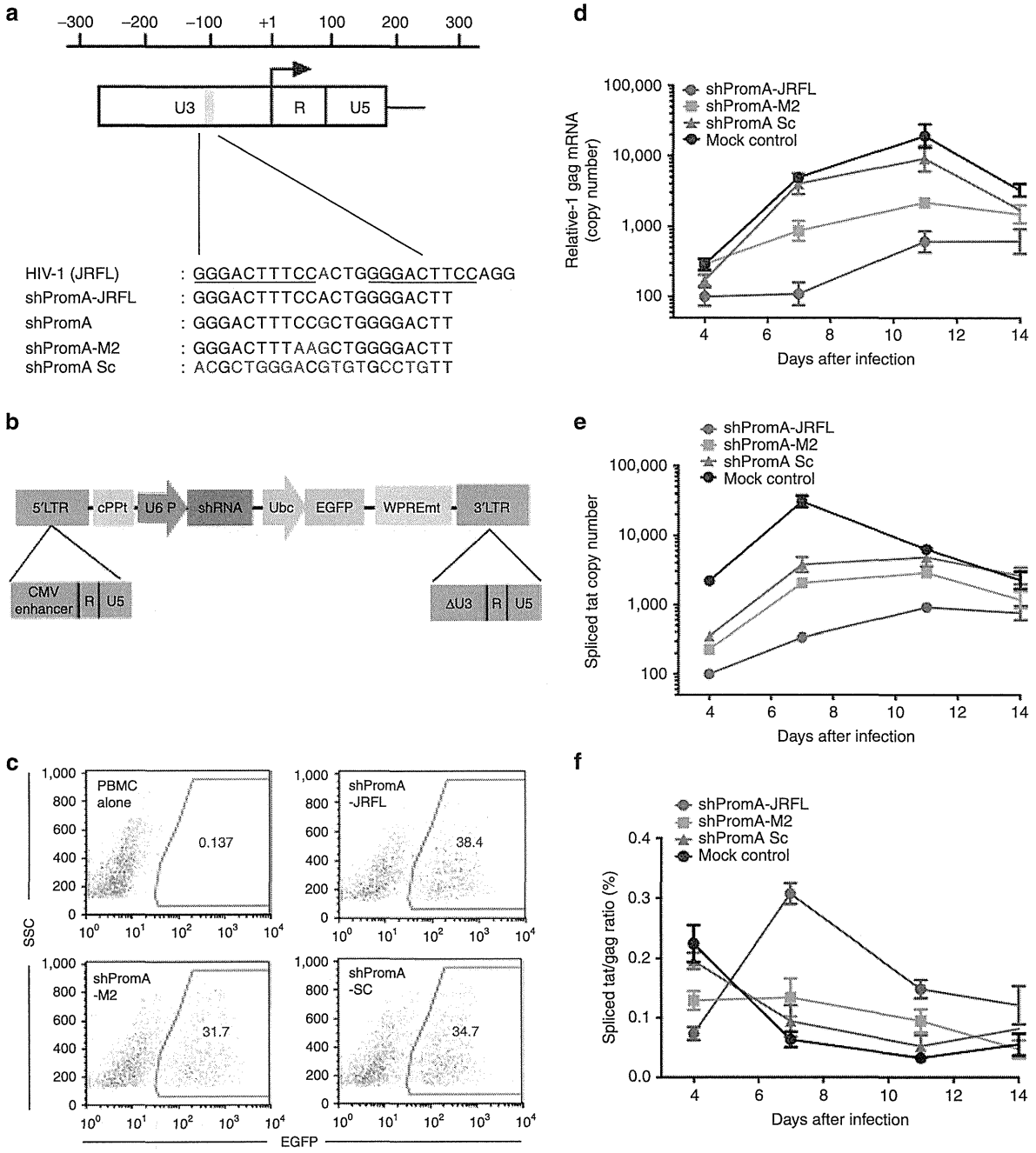

Figure 1 Human immunodeficiency virus (HIV)-1 transcription is inhibited by lenti-shPromA-JRFL in peripheral blood mononuclear cells (PBMCs). (**a**) Alignment of self-inactivating (SIN) lentivirus vector constructs along with HIV-1_{JRFL} target sequences. A map of HIV-1 5′ long terminal repeat (LTR) region is illustrated: the blue bar indicates the location of NF-κβ binding region; the arrow indicates the HIV-1 transcription start site; red text in the alignment highlights nucleic acids that differ from the HIV-1_{JRFL} sequence; numbers indicate the nucleic acid location relative to the transcription start site; and underlined text indicates NF-κβ binding region in the HIV-1 promoter. (**b**) Structure of SIN lentivirus vector. SIN vector consists of central polypurine tract (cPPT), U6 promoter (U6 P), short hairpin RNA (shRNA), ubiquitin C promoter (Ubc), and enhanced green fluorescent protein (EGFP). WPREmt, mutant woodchuck promoter response element, and modified LTR, allow integration but not expression of viral genome. We constructed U6 promoter–driven shRNA expression SIN lentivirus vector plasmid with EGFP expression unit targeting shPromA-JRFL, shPromA-M2 (three-base mismatched control), and shPromA-Sc (scramble control). (**c**) Expression of EGFP after transduction of lenti-shPromA, shM2, shSc into PBMCs. PBMCs prepared from a healthy donor were stimulated with interleukin-2 for 6 hours, followed by transduction of the lentivirus with a multiplicity of infection of 10. Five days later, EGFP expression was determined by flow cytometric analysis. (**d**) HIV-1 transcription is inhibited in PBMCs transduced by lenti-shPromA-JRFL. 2×10^6 transduced PBMCs were infected with 50 ng HIV-1_{JRFL}, as determined by the reverse transcriptase assay. The cell-associated HIV *gag* messenger RNA (mRNA) copy number normalized to 1,000 copies of GAPDH is shown along with time after HIV-1_{JRFL} infection. (**e**) HIV-1 spliced-*tat* expression is modulated in PBMCs transduced with lenti-shPromA-JRFL. Spliced-*tat* mRNA copy number normalized to 1,000,000 copies of GAPDH is shown following after HIV-1_{JRFL} infection. (**f**) The ratio of spliced-*tat* over unspliced HIV-1 mRNA, measured by HIV-1 *gag* mRNA, is shown following HIV-1_{JRFL} infection. In panels **d**, **e**, and **f** the mean values and SEM of three independent experiments are plotted.

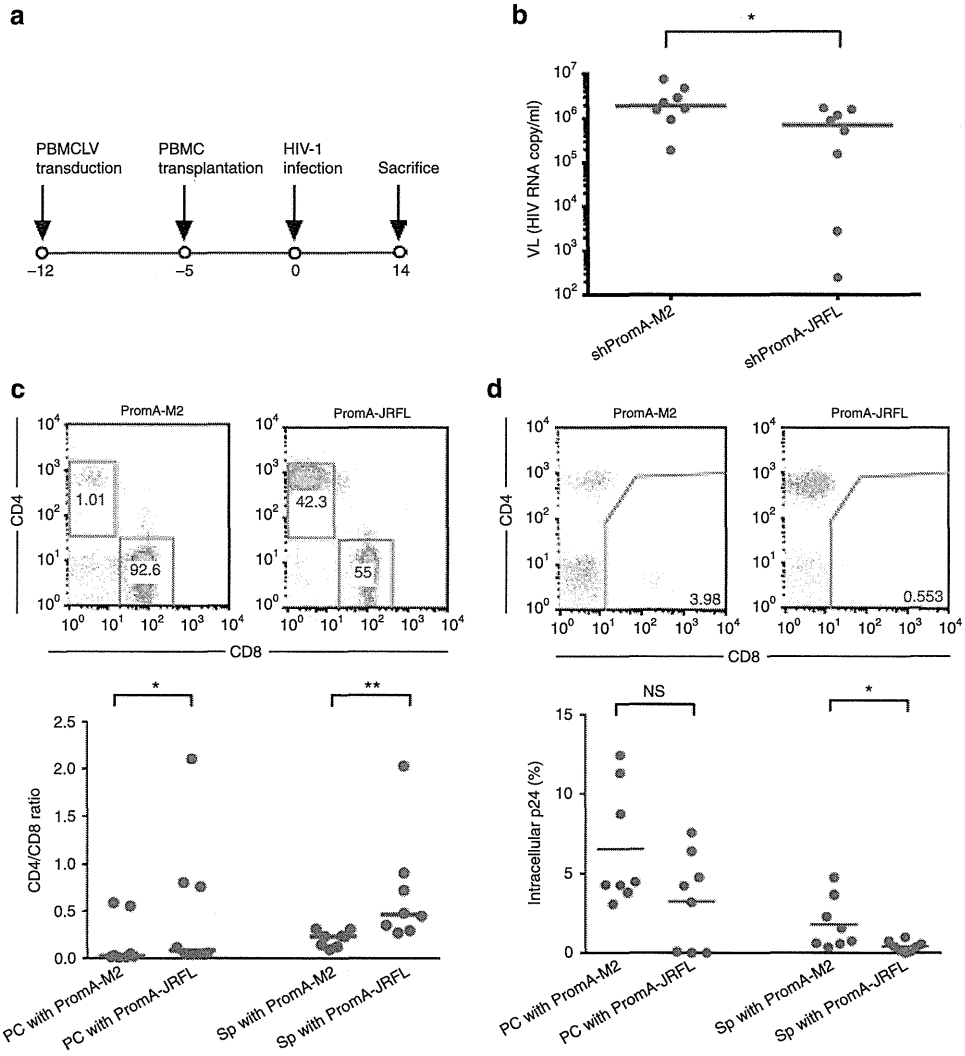

Figure 2 Transduction with lentivirus-shPromA-JRFL shows antiviral effects in NOJ mouse. (**a**) Time line for *in vivo* NOJ mouse experiment. LV denotes lentivirus. (**b**) Amount of viral load (VL) (HIV-1 RNA in serum) in mice with lentivirus-transduced peripheral blood mononuclear cells (PBMCs). Blood samples were collected from mice orbit on day 14 after HIV-1_{JRFL} infection. Horizontal bars indicate the medians. $^*P < 0.05$. (**c**) Effects on the ratio of $CD4^+/CD8^+$ cells in mice with lentivirus-transduced PBMCs. Short bars indicate the medians. $^*P < 0.05$, $^{**}P < 0.01$. (**d**) Effect on intracellular p24-positive cells. Peritoneal cavity cells and splenocytes recovered on day 14 after HIV-1 inoculation were analyzed by flow cytometry. The percentage of p24-positive cells among $CD4^+$ T cells (gated as $mCD45^-$ $hCD45^+$ $hCD3^+$ $hCD8^-$) is shown ($n = 8$). Horizontal bars indicate the medians. $^*P < 0.05$. NS, not significant; PC, peritoneal cavity; Sp, Spleen.

determine whether the degree of expression and processing of the shRNA constructs impacted the antiviral effects. It was found that the degree of antisense-strand expression had a strong inverse correlation with VL in serum in the mice transplanted with PromA-JRFL–transduced PBMCs ($r = 0.83$; $P = 0.0015$), but not in those transplanted with the control shRNA PromA-M2 (**Figure 3a**). Similarly, there was an inverse correlation between expression of cell-associated HIV-1 *gag* mRNA in $CD4^+$ T cells from the spleen and expression antisense strand of the shPromA-JRFL ($r = 0.84$; $P = 0.0014$; **Supplementary Figure S3a**) and strong linear correlation between VL and expression of cellular-associated HIV-1 *gag* mRNA in CD4 cells ($r = 0.84$; $P = 0.0014$; **Supplementary Figure S3b**). Consistent with these observations, there was a strong linear correlation between VL and both the percentage of p24-positive $CD3^+$ $CD8^-$ cells ($r = 0.98$; $P < 0.0001$; **Figure 3b**) and the cell-associated viral mRNA from splenocytes ($r = 0.84$; $P = 0.0014$) in shPromA-JRFL–expressing mice, indicating that serum VL correlates with cellular expression of HIV-1 Gag protein in $CD4^+$ T cells and *gag* mRNA in splenocytes. These data all point to the fact that the presence of the processed antisense strand of shPromA-JRFL is a strong correlate of inhibition of viral replication.

Phorbol myristate acetate, a strong stimulating reagent, reactivates silenced transcription of HIV-1 in *ex vivo* culture

Latent HIV-1 has silenced transcription, which is able to be switched on by strong cellular activating stimuli such as phorbol myristate acetate (PMA).[46] The U1 cell line is a latently infected monocytoid cell line that contains the proviral form of HIV-1, with heterochromatin formation in the viral promoter

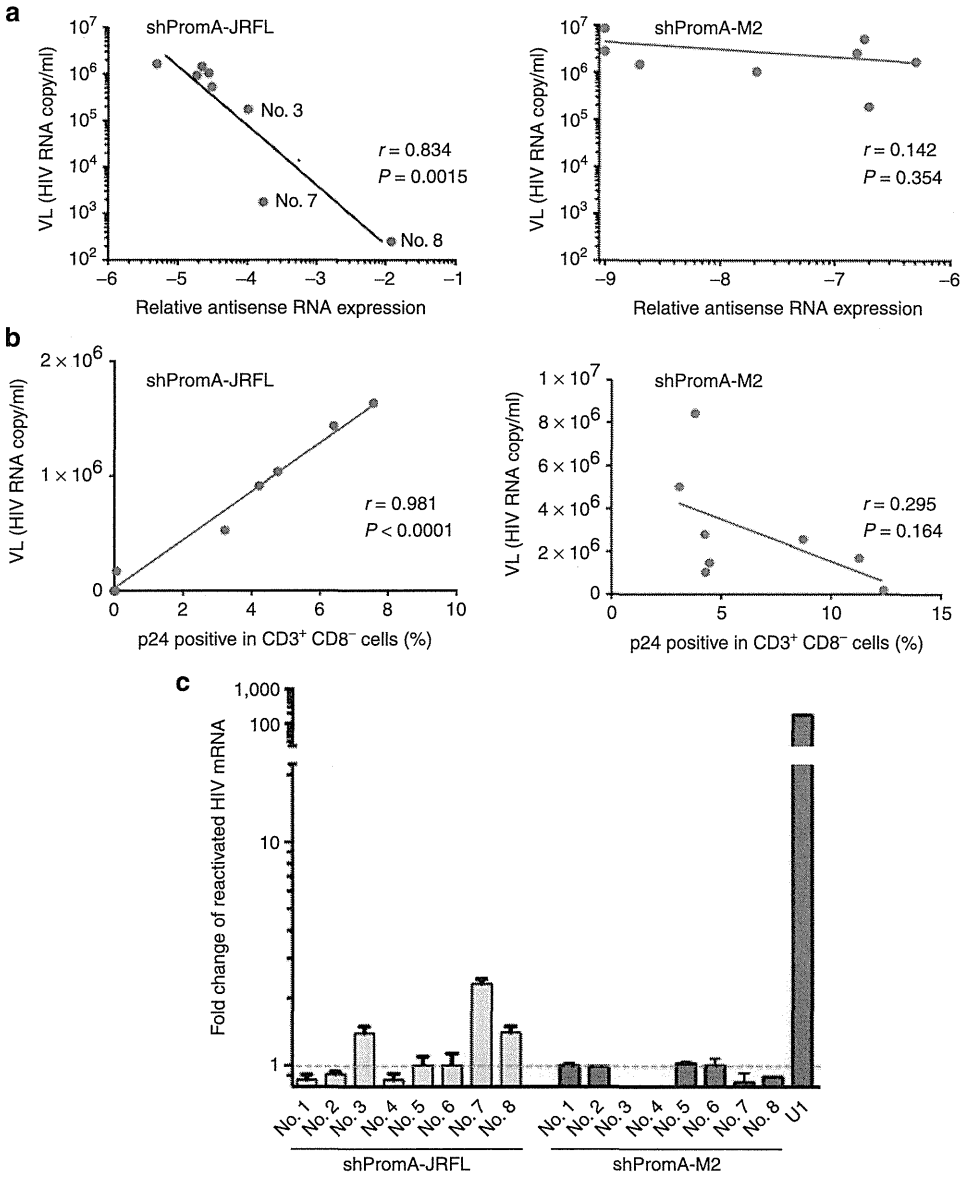

Figure 3 Transcriptional gene silencing (TGS) is induced by lenti-shPromA-JRFL. (**a**) Inverse correlation of expression level of the antisense strand of shPromA-JRFL and viral load (VL). Relative antisense RNA expression of shPromA-JRFL was detected by the primer-specific reverse transcriptase–polymerase chain reaction. (**b**) Linear correlation of intracellular p24 expression level and VL. Intercellular p24 staining in $CD3^+$ $CD8^-$ cells obtained from peritoneal cavity was analyzed by flow cytometry and was plotted against VL. (**c**) Transcriptionally suppressed human immunodeficiency virus (HIV)-1 is reactivated by phorbol myristate acetate (PMA). Splenocytes recovered from day 14 after inoculation of $HIV\text{-}1_{JRFL}$ were divided into two cultures with or without addition of PMA. After *ex vivo* culture for 24 hours, cellular-associated messenger RNA (mRNA) was extracted for analysis of HIV *gag* mRNA. Substantially increased expression of HIV-1 *gag* mRNA was found after PMA activation in three mice with highly suppressed HIV-1 (Nos. 3, 7, and 8), obtained from shPromA-JRFL treated mice. U1 is a positive control for HIV-1 latently infected cells. The mean values and SEM of three independent experiments are plotted.

region, the 5′LTR. The silenced provirus can be activated by treatment of cells with PMA with concomitant relaxation and opening of the chromatin structure.[47–49] Given that we have previously shown that si/shPromA acts by inducing biochemical changes in histone tails resulting in a heterochromatic structure associated with the 5′LTR, we hypothesized that the silenced HIV-1 induced by shPromA-JRFL would be activated by PMA. We conducted *ex vivo* culture of the splenic $CD4^+$ T cells from all mice in the shPromA-JRFL–treated group, including the three highly suppressed mice (nos. 3, 7, and 8, as indicated in Figure 3a). We found that PMA treatment resulted in elevated levels of *gag* mRNA in the PBMCs from the three suppressed mice, but not in those where VL was poorly suppressed. Of note, these were the same mice in which the antisense strand of shPromA-JRFL was poorly expressed (Figure 3c). We also found that PMA treatment did not increase the levels of *gag* mRNA in the PBMCs from the 8 mice treated with shPromA-M2 (Figure 3c). These data are consistent with TGS induced by shPromA-JRFL being responsible for the observed suppression of HIV-1 transcription.

We also confirmed the activation of HIV-1 transcription using an *in vitro* experimental model. We transduced PM1-CCR5 T cells, with lenti-shPromA-JRFL. We conducted limiting dilution of transduced PM1-CCR5 T cells to isolate strongly positive EGFP clonal populations (Figure 4a,b). After confirming expression of EGFP in more than 99% of cells in this clone, (PromA-JRFL No.3), we infected these cells with two concentrations of HIV-1_{JRFL} (Figure 4c). We also measured the expression level of the antisense strand of the shPromA-JRFL transcript by RT-qPCR in PM1-ccr5 cells in the presence of ongoing active HIV-1_{JRFL} infection. HIV infection did not make a difference to the expression levels of the antisense strand of the shPromA-JRFL transcript (**Supplementary Figure S4a,b**).[42] After confirming that shPromA-JRFL–expressing PM1-CCR5 cells completely suppressed HIV-1 replication, we then assessed whether activation of the suppressed HIV-1 transcription could be induced by various stimuli, including PMA and the histone deacetylase inhibitor, tricostatin A (Figure 4d). Both stimuli resulted in reactivation of viral replication, with tricostatin A having a greater effect than that of PMA. The powerful effect of tricostatin A in viral reactivation in the presence of shPromA-JRFL strongly suggests that this shRNA is causing viral suppression through TGS, because recruitment of histone deacetylase is a classic mark of TGS. It is interesting that not all activation stimuli result in reactivation of Prom-A–suppressed infection. GM-CSF stimulation of untransduced U1 cells results in reactivation of latent virus. However, GM-CSF stimulation of U1 cells lentivirally transduced to express shPromA did not result in increased viral replication (**Supplementary Figure S5**). These data are concordant with our previous *in vitro* data, demonstrating that siRNA and shPromA cause suppression of HIV-1 replication through TGS.[34,40,41] The data also suggest that TGS mediated through shRNA can be sustained even in the presence of certain cytokines, such as GM-CSF.

TGS induced by shPromA-JRFL was not associated with offtarget effects

Endosomal innate immune receptors, such as TLR3, TLR7, and TLR8, recognize long single- or double-stranded RNAs, triggering type I IFN and IFN-stimulated gene expression that can result in viral suppression by both nonspecific offtarget effects and undesirable toxicities.[37,38] We evaluated the extent of induction of IFN-α gene expression using RT-qPCR on splenocytes from shPromA-JRFL, shPromA-M2, and untreated mice. We used polyI:C (polyinosinepolycytosine)-treated PBMCs as a positive control.[50,51] There was no difference in IFN-α expression levels (Figure 5a). Furthermore, by RT-qPCR there was no difference in expression of the IFN-α response genes, OSA1, ISG20, and IFIT1 between groups of mice (Figure 5b), which is consistent with a lack of induction of IFN.

To exclude offtarget effects mediated through the targeting by shPromA-JRFL of other NF-κβ binding motifs of host genes as distinct from the NF-κβ motif in the HIV-1 LTR, a PCR-based assay was used to assess the expression levels of 86 NF-κβ-driven host genes, including IFN-α, β, and γ. The shPromA-JRFL was not associated with altered expression of NF-κβ driven host genes, including the IFN genes (**Supplementary Figure S6a,b**). These data are concordant

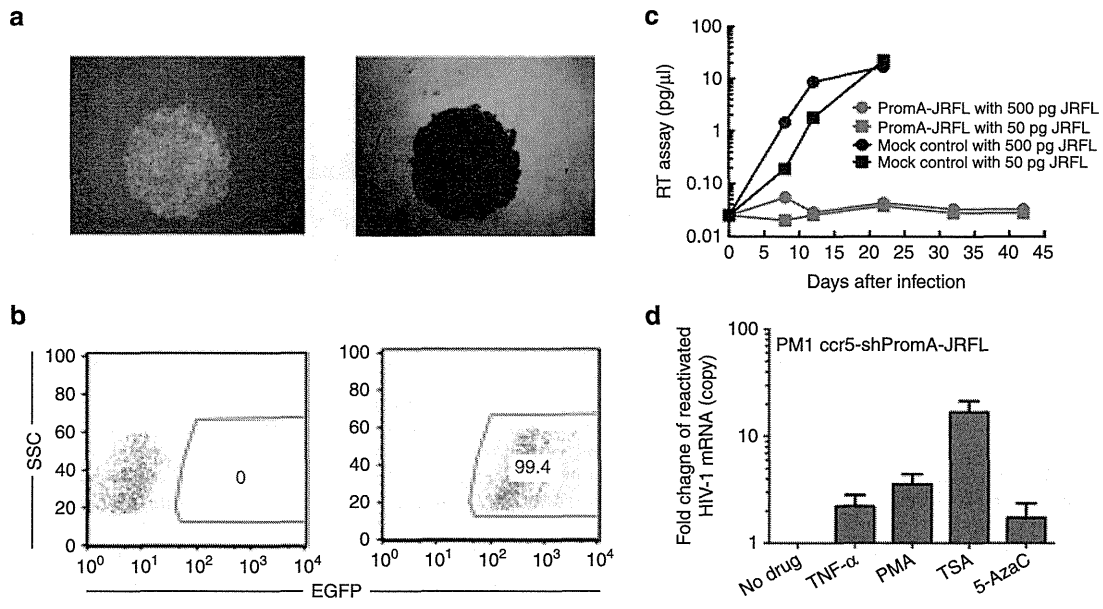

Figure 4 Transcriptional gene silencing (TGS) is induced by lenti-shPromA-JRFL *in vitro*. (**a**) PM1-ccr5 cells were transduced with lenti-shPromA with a multiplicity of infection of 10, subjected to limited dilution to isolate EGFP-positive colonies. A fluorescent image of clone PromA-JRFL No. 3. is shown on the left and the corresponding phase contrast image is on the right. (**b**) Expression of EGFP after expansion of clone PromA-JRFL No.3 as determined by flow cytometric analysis. (**c**) HIV-1 replication is inhibited in Lenti-shPromA-JRFL–transduced PM1-ccr5 cells. HIV-1 in the culture supernatant was detected by the colorimetric reverse transcriptase (RT) assay. (**d**) HIV-1 transcription is reactivated from the transcriptionally suppressed PM1-ccr5 cells, transduced with Lenti-shPromA-JRFL. 24 hours after activation with PMA or TSA, cell-associated mRNA was extracted for analysis of HIV *gag* mRNA. Fold change of reactivated HIV-1 *gag* mRNA is shown. 5Aza, 5-azacytidine; PMA, phorbol myristate acetate; TNF-α, tumor necrosis factor-α; TSA, trichostatin A. The mean values and SEM of three independent experiments are plotted.

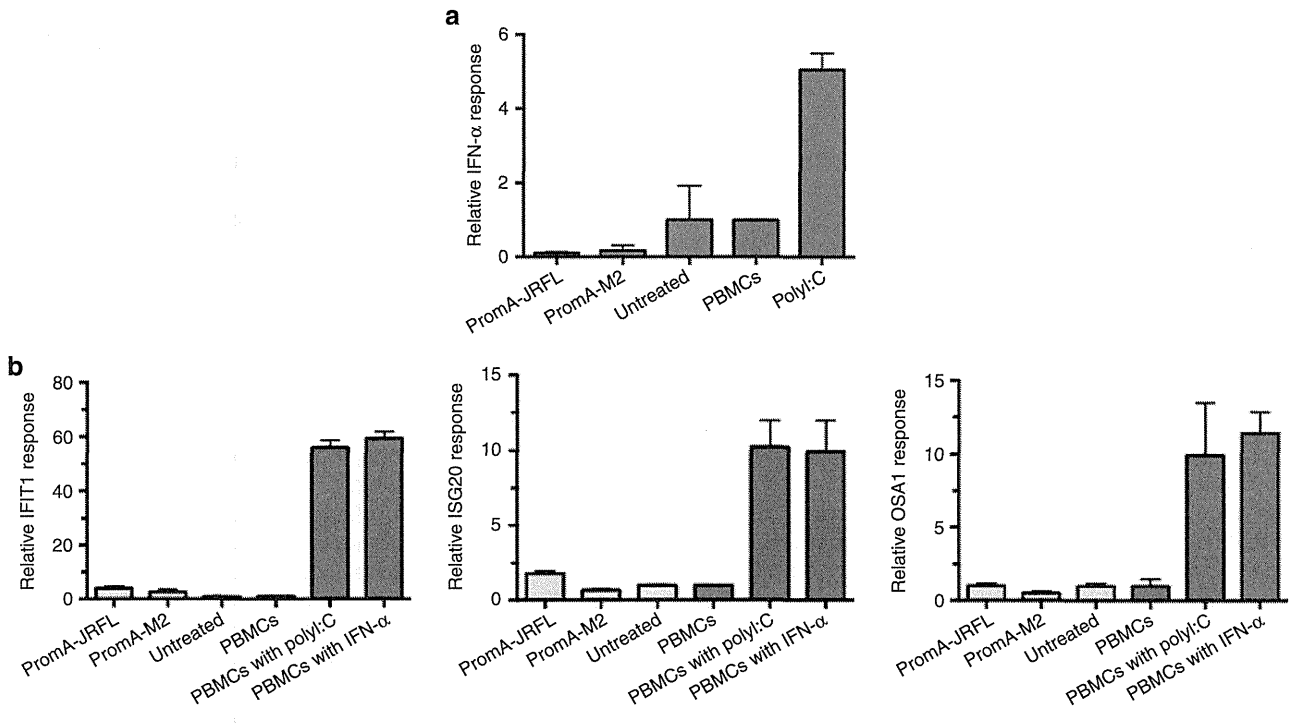

Figure 5 No significant offtarget effects are induced by lenti-shPromA-JRFL. (**a**) Effect of lentiviral transduction of peripheral blood mononuclear cells (PBMCs) on interferon-α (IFN-α) expression. Splenocytes were prepared from mice transplanted with lentivirus-transduced PBMCs. Cell-associated messenger RNA (mRNA) was extracted for analysis of IFN-α by reverse transcriptase–polymerase chain reaction (RT-PCR). PolyI:C–treated PBMCs were used a positive control, indicated in dark blue. (**b**) Effect of lentiviral transduction of PBMCs on IFN response genes. Cell-associated mRNA was extracted for analysis of three IFN-α response genes (OSA1, ISG20, and IFITM1) by RT-PCR. PolyI:C or IFN-α–treated PBMCs were used as positive controls, these are indicated in dark blue. The mean values and SEM of three independent experiments are plotted.

to our previous analyses of offtarget effects induced by siRNA and shRNA forms of PromA in HeLa and MOLT-4 cell and strongly suggest that the observed HIV-1 suppression is not the result of offtarget effects induced by shPromA-JRFL.[42]

Discussion

Our previous *in vitro* data based on HeLa or T-cell lines suggested that TGS of HIV-1 can be induced by promoter targeted si/shRNAs through the induction of epigenetic modifications to form heterochromatin structures, which resemble the biochemical modifications of the HIV-1 promoter in latently infected cell lines.[12,13] In this report, we extend our si/shRNA-mediated TGS approach into an *in vivo* NOJ humanized mouse model.[43] Although there are several reports of PTGS mediated by siRNA using *in vivo* humanized mouse models,[50–54] this report demonstrates that HIV-1 gene silencing based on the TGS pathway is possible *in vivo*. Our NOJ model is a model of acute rapidly progressive HIV infection in which massive infection occurs: hCD4/CD8 cell ratio significantly decreases, and high VL is achieved within 14 days of intraperitoneal inoculation of $HIV\text{-}1_{JRFL}$.[43] Despite this highly activated, destructive, and rapidly progressive infection with high levels of viral transcription, we were still able to successfully demonstrate a degree of viral suppression using an shRNA that induces transcriptional silencing.

We demonstrated substantial antiviral effects that resulted in significant alterations in a number of surrogate markers of disease progression in the shPromA-JRFL–treated group, including reduced serum VL, reduced percentage of HIV Gag p24 protein–positive $CD3^+$ $CD8^-$ T cells, and an improved ratio of $CD4^+/CD8^+$ T cells. Of note, the extent of each of these effects correlated with the extent of expression of the processed shRNA antisense strand. These data also suggest that in mice that showed adequate expression of the antisense strand of shPromA-JRFL in $CD4^+$ T cells, there was an observable HIV-1 antiviral effect, which we conclude is occurring through TGS. Because the $CD4^+$ T cells were relatively protected from active HIV-1 infection through shPromA-JRFL–mediated TGS, we could see significant reduction of VL in serum in shPromA-JRFL mice. The data from the *in vitro* PBMC experiments show that shPromA-JRFL has marked effects on production of both spliced and unspliced viral mRNA. Reduction in the production of spliced-*tat* is likely to be important in the effective silencing of latently infected cells, as Tat, through its interaction with the TAR region of the 5′LTR allows efficient upregulation of transcription of long unspliced HIV-1 mRNA.[55–57] Furthermore, the *ex vivo* reactivation of HIV-1 infection by PMA stimulation is consistent with our previously reported observations that siPromA and shPromA constructs result in viral suppression by TGS[40,41] and with other models of HIV-1 latency.[47–49,58] In addition, the *ex vivo* reversal of viral suppression by TNF-α and, in particular, by the histone deacetylase inhibitor, tricostatin A, is consistent with suppression being induced by TGS. We confirmed that shPromA-JRFL did not induce any significant offtarget effects, determined by expression of type

I and II IFNs, IFN response genes and NF-κβ–regulated host genes. We also demonstrated that not all activating stimuli reverse this process, for example, the GM-CSF–induced activation of latent HIV-1 in shPromA–transduced U1 cell was inhibited.

This acute human PBMC-NOJ mouse model has been used to demonstrate proof of principle of potential *in vivo* efficacy of shPromA delivered by a retroviral vector, focusing on the relative protection of human CD4+ T cells against HIV-1 infection. To further this approach, we are investigating the use of newborn NOJ mouse engrafted via intrahepatic injection of human cord blood–derived CD34+ cells transduced with retroviral constructs expressing shPromA and appropriate controls.[59] This will enable us to evaluate the effect of this approach on engraftment and hematopoietic cell differentiation and reconstitution, and subsequently on HIV-1 infection. An advantage of the CD34+ NOJ model is that the cell number required in this model is 100-fold lower (5×10^4 CD34+ cells per mouse) than that of required in the current NOJ mouse model reconstituted by human PBMCs (1×10^7 PBMCs per mouse). The titer of our current lentiviruses is ~2×10^8 infectious viral particle per milliliter. Therefore, a higher multiplicity of infection can be achieved to obtain a greater transduction rate, which will potentially provide greater efficacy.

Using the CD34+ cell–reconstituted NOJ model, we wish to explore a scenario closer to that which we envisage these constructs will be used in human HIV-1 treatment, primarily on cessation of antiretroviral drugs in controlled chronic infection to determine whether lentivirally delivered shPromA constructs can stabilize the viral reservoir on withdrawal of antiretroviral therapy. If the latent viral reservoir could be maintained as effectively silenced by shPromA treatment, these constructs would represent a substantial step forward on the road toward a functional cure, by providing an alternative to the currently proposed eradication strategies than using various viral transcription activating agents, such as histone deacetylase and demethylases.[49,60,61] Rather than activating virus and abolishing infected cells, we propose that constructs such as shPromA could be used to lock HIV-1 into latency maintaining transcriptionally inactive virus even in patients ceasing conventional antiretroviral therapy, thus achieving a prolonged remission or functional cure of HIV-1 infection.

Materials and methods

Production of lentivirus. The construction of lentiviral vector lenti-shPromA-JRFL, lenti-shPromA-M2, and lenti-Sc were previously described.[41] An outline of the construction of self-inactivated lentivirus vector plasmid with GFP expression unit is illustrated in **Figure 1b**. Vesicular stomatitis virus-G (VSV-G) pseudotyped lentiviral vectors were prepared by transduction of plasmid DNA into 293T cells using HilyMax (Dojindo Molecular Technologies, Osaka, Japan), a lipofectamine-based transfection reagent. The resulting virus was concentrated from supernatant as previously described[62,63], and stocks were titrated on 293T cells based on EGFP expression.

PBMC transduction with lentivirus. Peripheral blood was collected from healthy volunteers after informed consent was obtained, according to the institutional guidelines approved by the Faculty of Life Sciences and Pharmaceutical Sciences, Kumamoto University, Kumamoto, Japan. Healthy donor PBMCs were prepared by standard density gradient centrifugation using Ficoll-Hypaque (VWR, Murarrie, Australia). Cells were cultured in RPMI-1640 medium supplemented with penicillin (100 U/ml), streptomycin (100 µg/ml), 20% fetal calf serum (R20) in the presence of 20 units/ml of interleukin-2 (Roche Diagnostic, Castle, Hill, Australia) for 7 hours, followed by overnight transduction with either lenti-shPromA-JRFL, lenti-shPromA-Sc, or lenti-shPromA-M2 using a multiplicity of infection of 1.5–2.0. Cells were then cultured in R20 for a further 7 days before transplantation.

Transplantation of human PBMCs into NOJ mice and HIV-1 infection of mice. Human PBMC-transplanted NOJ (hu-PBMC-NOJ) mice were generated as described previously.[43] Briefly, NOJ mice were irradiated (1.0 Gy), and bulk lenti-shPromA-JRFL– or lenti-shPromA-M2–transduced PBMCs (1×10^7) were resuspended in phosphate-buffered saline (PBS) (0.1 ml) and infused intraperitoneally into each mouse. Seven days after PBMC implantation, a dose of 200 ng of HIV-1_{JRFL}, which was determined by HIV-1 p24 antigen ELISA (ZeproMetrix), suspended in 0.1 ml of PBS, was inoculated intraperitoneally into each mouse. On day 14 after HIV-1_{JRFL} infection, mice were killed and blood samples were collected from the mouse orbit, and peritoneal cavity and spleen cells were harvested and resuspended in PBS (see **Figure 2a**). All animal experiments were performed according to the guidelines of the Kumamoto University Graduate School of Medical Science.

RT-PCR analysis and RT assay. Cellular RNA was extracted using High Pure RNA Tissue Kit (Roche Diagnostic), followed by the RT-PCR analysis as described previously.[39,42] Detection of spliced-*tat* was conducted using the same RT-PCR conditions with the primer set: Tat-F: ATG GAG CCA GTA GAT CCT AGA CTA and Tat-B: ATT CCT TCG GGC CTG TCG using RT-PCR (SensiFAST Probe one-step RT-PCR: Bioline). Both HIV-1 *gag* mRNA and spliced-*tat* mRNA levels were normalized against GAPDH. Colorimetric RT activity (RT assay) in culture supernatants was determined as previously described.[64]

Flow analysis of CD4+ CD8+ T cells and internal p24 staining. Lymphocyte subsets from human mononuclear cells obtained from the transplanted mice were characterized by flow cytometric analysis as described previously.[43] Briefly, cells were treated with red cell lysing buffer (155 mM NH_4Cl, 10 mM $KHCO_3$, and 0.1 mM EDTA) to lyse erythrocytes, and single-cell suspensions were prepared in staining medium (PBS with 2% fetal bovine serum and 0.05% sodium azide) and stained with monoclonal antibodies: allophycocyanin (APC)-Cy7–conjugated antimouse CD45 (BD Pharmingen, Kobe, Japan), APC-conjugated anti-hCD4 (Dako, Tokyo, Japan), phycoerythrin-Cy7–conjugated anti-hCD3 (e-Bioscience, Tokyo, Japan), Pacific Blue–conjugated anti-hCD8 (BioLegend, Tokyo, Japan), and Pacific Orange–conjugated antihuman CD45 (anti-hCD45) (Invitrogen, Tokyo, Japan). After 30 minutes, cells were washed twice and fixed in PBS with 1% paraformaldehyde for 20 minutes and permeabilized in PBS with 0.1% saponin. After a 10-minute incubation, cells were

stained with phycoerythrin-conjugated anti-HIV-1 p24 monoclonal antibody (Beckman Coulter, Tokyo, Japan) for 30 minutes. All washes and staining procedures were conducted at 4 °C. Following staining, the cells were analyzed on an LSR II flow cytometer (BD Bioscience). Data were analyzed with FlowJo software (Tree Star, Tokyo, Japan).

Statistical analysis. RT-PCR analysis and RT assay values are given as mean and SEM. Ratio of $CD4^+/CD8^+$ cells and VL were tested for significance using a nonparametric Mann–Whitney *U* test. A *P* value <0.05 was considered statistically significant. All analyses were performed using GraphPad Prism Version 5.0a (Graphpad Software, San Diego, CA).

Supplementary material

Figure S1. Effects of lenti-shPromA-JRFL and lenti-shPromA-M2 on $CD4^-$ T cells.
Figure S2. Effects of lenti-shPromA-JRFL and lenti-shPromA-M2 on $CD8^+$ T cells.
Figure S3. HIV-1 gag HIV mRNA level is inhibited through TGS induced by lenti-shPromA-JRFL.
Figure S4. The antisense strand expression level is not altered with HIV-1JRFL infection.
Figure S5. Activation of latent HIV-1–infected U1 cells is inhibited by lenti-shPromA.
Figure S6. No significant difference in comparison of 86 NF-κβ driven genes in PBMCs trasduced with lenti-shPromA.

Acknowledgments. The authors thank the Australian Government Department of Health and Ageing (RM07292) and National Health and Medical Research Council (455350 to A.K. and 630571 for K.S. and C.H.). Funding for open-access charge was provide by St. Vincent's Centre for Applied Medical Research.

1. Ho, DD, Neumann, AU, Perelson, AS, Chen, W, Leonard, JM and Markowitz, M (1995). Rapid turnover of plasma virions and CD4 lymphocytes in HIV-1 infection. *Nature* **373**: 123–126.
2. Mellors, JW, Rinaldo, CR Jr, Gupta, P, White, RM, Todd, JA and Kingsley, LA (1996). Prognosis in HIV-1 infection predicted by the quantity of virus in plasma. *Science* **272**: 1167–1170.
3. Perelson, AS, Essunger, P, Cao, Y, Vesanen, M, Hurley, A, Saksela, K *et al.* (1997). Decay characteristics of HIV-1-infected compartments during combination therapy. *Nature* **387**: 188–191.
4. Palella, FJ Jr, Delaney, KM, Moorman, AC, Loveless, MO, Fuhrer, J, Satten, GA *et al.* (1998). Declining morbidity and mortality among patients with advanced human immunodeficiency virus infection. HIV Outpatient Study Investigators. *N Engl J Med* **338**: 853–860.
5. Chun, TW, Finzi, D, Margolick, J, Chadwick, K, Schwartz, D and Siliciano, RF (1995). *In vivo* fate of HIV-1-infected T cells: quantitative analysis of the transition to stable latency. *Nat Med* **1**: 1284–1290.
6. Finzi, D, Hermankova, M, Pierson, T, Carruth, LM, Buck, C, Chaisson, RE *et al.* (1997). Identification of a reservoir for HIV-1 in patients on highly active antiretroviral therapy. *Science* **278**: 1295–1300.
7. Siliciano, RF and Greene, WC (2011). HIV latency. *Cold Spring Harb Perspect Med* **1**: a007096.
8. Wong, JK, Hezareh, M, Günthard, HF, Havlir, DV, Ignacio, CC, Spina, CA *et al.* (1997). Recovery of replication-competent HIV despite prolonged suppression of plasma viremia. *Science* **278**: 1291–1295.
9. Chun, TW, Justement, JS, Moir, S, Hallahan, CW, Maenza, J, Mullins, JI *et al.* (2007). Decay of the HIV reservoir in patients receiving antiretroviral therapy for extended periods: implications for eradication of virus. *J Infect Dis* **195**: 1762–1764.
10. Turner, AM, De La Cruz, J and Morris, KV (2009). Mobilization-competent Lentiviral Vector-mediated Sustained Transcriptional Modulation of HIV-1 Expression. *Mol Ther* **17**: 360–368.
11. Malecová, B and Morris, KV (2010). Transcriptional gene silencing through epigenetic changes mediated by non-coding RNAs. *Curr Opin Mol Ther* **12**: 214–222.
12. Suzuki, K and Kelleher, AD (2009). Transcriptional regulation by promoter targeted RNAs. *Curr Top Med Chem* **9**: 1079–1087.
13. Suzuki, K and Kelleher, AD. (2010). Lessons from viral latency in T cells: manipulating HIV-1 transcription by siRNA. *HIV Therapy* **4**: 199–213.
14. Ahlenstiel, CL, Lim, HG, Cooper, DA, Ishida, T, Kelleher, AD and Suzuki, K (2012). Direct evidence of nuclear Argonaute distribution during transcriptional silencing links the actin cytoskeleton to nuclear RNAi machinery in human cells. *Nucleic Acids Res* **40**: 1579–1595.
15. Knowling, S, Stapleton, K, Turner, AM, Uhlmann, E, Lehmann, T, Vollmer, J *et al.* (2012). Chemically Modified Oligonucleotides Modulate an Epigenetically Varied and Transient Form of Transcription Silencing of HIV-1 in Human Cells. *Mol Ther Nucleic Acids* **1**: e16.
16. Turner, AM, Ackley, AM, Matrone, MA and Morris, KV (2012). Characterization of an HIV-targeted transcriptional gene-silencing RNA in primary cells. *Hum Gene Ther* **23**: 473–483.
17. Turunen, MP, Lehtola, T, Heinonen, SE, Assefa, GS, Korpisalo, P, Girnary, R *et al.* (2009). Efficient regulation of VEGF expression by promoter-targeted lentiviral shRNAs based on epigenetic mechanism: a novel example of epigenetherapy. *Circ Res* **105**: 604–609.
18. Novina, CD, Murray, MF, Dykxhoorn, DM, Beresford, PJ, Riess, J, Lee, SK *et al.* (2002). siRNA-directed inhibition of HIV-1 infection. *Nat Med* **8**: 681–686.
19. Jacque, JM, Triques, K and Stevenson, M (2002). Modulation of HIV-1 replication by RNA interference. *Nature* **418**: 435–438.
20. Boden, D, Pusch, O, Lee, F, Tucker, L and Ramratnam, B (2003). Human immunodeficiency virus type 1 escape from RNA interference. *J Virol* **77**: 11531–11535.
21. Das, AT, Brummelkamp, TR, Westerhout, EM, Vink, M, Madiredjo, M, Bernards, R *et al.* (2004). Human immunodeficiency virus type 1 escapes from RNA interference-mediated inhibition. *J Virol* **78**: 2601–2605.
22. von Eije, KJ, ter Brake, O and Berkhout, B (2008). Human immunodeficiency virus type 1 escape is restricted when conserved genome sequences are targeted by RNA interference. *J Virol* **82**: 2895–2903.
23. Westerhout, EM, Ooms, M, Vink, M, Das, AT and Berkhout, B (2005). HIV-1 can escape from RNA interference by evolving an alternative structure in its RNA genome. *Nucleic Acids Res* **33**: 796–804.
24. Shah, PS, Pham, NP and Schaffer, DV (2012). HIV develops indirect cross-resistance to combinatorial RNAi targeting two distinct and spatially distant sites. *Mol Ther* **20**: 840–848.
25. ter Brake, O, Konstantinova, P, Ceylan, M and Berkhout, B (2006). Silencing of HIV-1 with RNA interference: a multiple shRNA approach. *Mol Ther* **14**: 883–892.
26. Wassenegger, M, Heimes, S, Riedel, L and Sänger, HL (1994). RNA-directed de novo methylation of genomic sequences in plants. *Cell* **76**: 567–576.
27. Wassenegger, M (2000). RNA-directed DNA methylation. *Plant Mol Biol* **43**: 203–220.
28. Mette, MF, Matzke, AJ and Matzke, MA (2001). Resistance of RNA-mediated TGS to HC-Pro, a viral suppressor of PTGS, suggests alternative pathways for dsRNA processing. *Curr Biol* **11**: 1119–1123.
29. Jones, L, Ratcliff, F and Baulcombe, DC (2001). RNA-directed transcriptional gene silencing in plants can be inherited independently of the RNA trigger and requires Met1 for maintenance. *Curr Biol* **11**: 747–757.
30. Sibley, CR, Seow, Y and Wood, MJ (2010). Novel RNA-based strategies for therapeutic gene silencing. *Mol Ther* **18**: 466–476.
31. Roberts, TC, Andaloussi, SE, Morris, KV, McClorey, G and Wood, MJ (2012). Small RNA-Mediated Epigenetic Myostatin Silencing. *Mol Ther Nucleic Acids* **1**: e23.
32. Miller, V and Larder, BA (2001). Mutational patterns in the HIV genome and cross-resistance following nucleoside and nucleotide analogue drug exposure. *Antivir Ther (Lond)* **6**(suppl. 3): 25–44.
33. Klenerman, P, Wu, Y and Phillips, R (2002). HIV: current opinion in escapology. *Curr Opin Microbiol* **5**: 408–413.
34. Suzuki, K, Juelich, T, Lim, H, Ishida, T, Watanebe, T, Cooper, DA *et al.* (2008). Closed chromatin architecture is induced by an RNA duplex targeting the HIV-1 promoter region. *J Biol Chem* **283**: 23353–23363.
35. Weinberg, MS, Barichievy, S, Schaffer, L, Han, J and Morris, KV (2007). An RNA targeted to the HIV-1 LTR promoter modulates indiscriminate off-target gene activation. *Nucleic Acids Res* **35**: 7303–7312.
36. Jackson, AL, Bartz, SR, Schelter, J, Kobayashi, SV, Burchard, J, Mao, M *et al.* (2003). Expression profiling reveals off-target gene regulation by RNAi. *Nat Biotechnol* **21**: 635–637.
37. Hornung, V, Guenthner-Biller, M, Bourquin, C, Ablasser, A, Schlee, M, Uematsu, S *et al.* (2005). Sequence-specific potent induction of IFN-alpha by short interfering RNA in plasmacytoid dendritic cells through TLR7. *Nat Med* **11**: 263–270.
38. Judge, AD, Sood, V, Shaw, JR, Fang, D, McClintock, K and MacLachlan, I (2005). Sequence-dependent stimulation of the mammalian innate immune response by synthetic siRNA. *Nat Biotechnol* **23**: 457–462.
39. Suzuki, K, Shijuuku, T, Fukamachi, T, Zaunders, J, Guillemin, G, Cooper, D *et al.* (2005). Prolonged transcriptional silencing and CpG methylation induced by siRNAs targeted to the HIV-1 promoter region. *J RNAi Gene Silencing* **1**: 66–78.
40. Lim, HG, Suzuki, K, Cooper, DA and Kelleher, AD (2008). Promoter-targeted siRNAs induce gene silencing of simian immunodeficiency virus (SIV) infection *in vitro*. *Mol Ther* **16**: 565–570.
41. Yamagishi, M, Ishida, T, Miyake, A, Cooper, DA, Kelleher, AD, Suzuki, K *et al.* (2009). Retroviral delivery of promoter-targeted shRNA induces long-term silencing of HIV-1 transcription. *Microbes Infect* **11**: 500–508.